Lubricating properties of fuel oils: quantification of lubricity.

T Thobejane

Lubricating properties of fuel oils: quantification of lubricity.

T Thobejane

13121261

Department of Chemical Engineering

University of Pretoria

Lubricating properties of fuel oils: quantification of lubricity.

Abstract

Asphaltenes are components of heavy fuel oils with complex aromatic structures containing heteroatoms (N, O, S) and metals (V, Fe, Ni) and contribute to the high viscosity of heavy fuel oils. Fuel oils are passed through pumps, filters, nozzles and other equipment before such fuel oils reach the burner section and therefore require good lubricating properties. In the recent past, several users of fuel oils have been experiencing problems such as blockages in the fuel oil filters and injector nozzles, increased wear and failures of pumps and, in some cases, decreased calorific efficiency of combustion. The high frequency reciprocating rig (HFRR) lubricity tester (method ISO 12156-1) was used to perform lubricity tests on fuel oil samples at different temperatures and atmospheric conditions to obtain a better understanding of the friction and wear behaviour of fuel oils. Three fuel oil samples with different asphaltene concentrations were selected for this purpose. These fuel oils were namely: a light cycle oil (LFO), a medium wax-blend oil (MFO) and a crude-derived heavy fuel oil (HFO). In an attempt to understand the role of oxygen as a contributing cause of the problems experienced with fuel oils at different temperatures, two atmospheres (i.e. oxygen-rich (atmospheric air) and inert (nitrogen)) were used to perform the lubricity tests.

Results indicate that the presence of asphaltenes changes the viscosity behaviour of fuel oils, which, in turn affects the lubricity behaviour. LFO with no asphaltenes (solid particles only) has little impact on the coefficient of friction and wear from 60 to 115 °C. MFO containing high molecular weight paraffin (wax), low concentrations of asphaltenes and solid particles results in a more stable fuel oil, resulting in less friction and wear and good high temperature performance. HFO containing high concentrations of asphaltenes and solid particles results in very high coefficient of friction (COF) and severe abrasive wear at high temperatures. At low and moderate temperatures, unfiltered HFO performs comparable to filtered HFO without asphaltenes and solid particles. Key performance indicators like the wear scar diameter on the ball as well as the wear track on the test ball, showed unexpected results indicating that temperature and atmospheric conditions contribute to the friction and wear behaviour of the fuel oils, but that composition of each of these fuel oils

played a significant role. For MFO, at high temperatures, wear increases drastically under nitrogen atmosphere when compared with oxygen-rich atmosphere. For HFO, the high concentration of asphaltenes content results in minimal change in the COF and wear with a change in environmental atmosphere. The poor lubricity of HFO is predominantly due to the asphaltenes and solid particles in HFO.

Keywords: Friction, wear, lubricity, oxygen, asphaltenes, fuel oils.

Contents

Nomenclature

Symbol	Description	Units
AVP	Absolute vapour pressure	kPa
CCAI	Calculated carbon aromaticity index	dimensionless
CR	Complementary rating	Dimensionless
COF	Coefficient of friction	dimensionless
DM	Distillate Marine	-
DF	Distillate fatty acid methyl esters	-
ECR	Electrical contact resistance	%
F	Frictional force	N
FAME	Fatty acid methyl esters	-
HCF	Humidity correction factor	$\mu m(kPa)^{-1}$
HCO	Heavy cycle oil	mL
HFO	Heavy fuel oil	mL
HFRR	High frequency reciprocating rig	-
ICP-OES	Inductively coupled plasma-optical emission spectrometry	-
KF	Karl Fischer	-
Kv	Kinematic viscosity	$mm^2(s)^{-1}$
K_w	Wear coefficient	$mm^3(Nm)^{-1}$
L	Sliding distance	m
LFO	Light cycle oil	mL
LCO	Light cycle oil	mL
MFO	Medium wax-blend oil	mL
N	Normal force	N
P_s	Saturation vapour pressure	kPa
P_w	Partial pressure	kPa
RH	Relative humidity percentage	%
RM	Residual marine	-
T	Temperature	°C
V	Wear Volume	m^3
V_{KF}	Consumption of titrant	mL

W	Load	N
WAT	Wax appearance temperature	°C
WC	Water content	%
W_{eq}	Titer of the titrant	mg
W_{sample}	Weight of sample	mg
$WS_{1.4}$	Corrected wear scar diameter	μm
WSD	Wear scar diameter	μm
X	wear scar perpendicular to the oscillation direction	μm
Y	wear scar parallel to the oscillation direction	μm

Greek

Symbol	**Description**	**Units**
μ	Coefficient of friction	dimensionless
ρ_{15}	Density at 15 °C	$Kg(m)^{-3}$

1. Introduction, Aims and Objectives

Fuel oils are passed through pumps, filters, nozzles and other equipment which require good lubricating properties before they reach the burner section. In recent past, several users of fuel oils are experiencing problems such as blockages in the fuel oil filters and injector nozzles, increased wear and failures of pumps and, in some cases, decreased calorific efficiency of combustion. These problems appear to be linked to the fuel oil chemical and physical properties which make up their composition. The most prominent problematic part of the composition appears to be the presence of asphaltenes (Kirk, 2015). These above problems and their causes stand to be confirmed and addressed in a way that will also help to improve the current fuel oil requirements for industrial use. The aim of this investigation is to determine the lubricating properties of fuel oils by focusing on the friction and wear capabilities of fuel oil taking into account presence of asphaltenes in the fuel oils, the composition of the fuel oils and presence of an oxidising atmosphere. The objective of this investigation is to perform friction and wear tests for the filtered and unfiltered fuel oils at different temperatures and chamber atmospheres using a HFRR tribometer. The fuel oil samples were provided by Sasol.

Severely-loaded systems such as nozzles, injectors or pumps require fuels with high lubricity to avoid wear problems (Lapuerta *et al*, 2016). Poor lubricants have a potential for causing premature wear which leads to high repair costs and failure of pumps (Nickels, 2011). Friction reduction and wear control is thus of particular importance for economic reasons and long term reliability of equipment (Bhushan, 2013: 4)

Fuel oils comprise of a range of liquid combustibles, mainly hydrocarbons, which are obtained either as distillates in the working up of petroleum or as residues after the lighter fractions have been removed (Harker & Allen, 1972: 120). Properties of heavy (residual) fuel oils show that the polar fractions, including asphaltenes, are likely to be irreversibly adsorbed onto a metal surface and are less resistant to oxidation as compared to paraffins because of their polarity (Ghanavati *et al*, 2013; Garaniya *et al,* 2018; Stachowiak & Batchelor, 2014: 38). Experimental results from a study, where asphaltenes were removed from heavy fuel oils and then added back to the maltenes (saturates, aromatics and resins), indicate that viscosity of the reconstituted heavy fuel

oil samples increases exponentially as the asphaltene content increases at constant temperature (Ghanavati *et al*, 2013). Distillate fuel oils can be used as a blending component in heavy fuel oil for viscosity adjustments in order to reduce the final viscosity of heavy fuel oil (Cao *et al*, 2021).

This investigation is focused on fuel oil used in industrial burners in order to obtain a fuel oil benchmark to quantify lubricity of the fuel oils in a similar way to other liquid products, for which standardised lubricity specifications exist. The aim of this investigation was thus to determine the lubricating properties of fuel oils used in power generation by focusing on their friction and wear capabilities, whilst also taking into consideration the effect of the presence of asphaltenes in fuel oils and the effect of oxidative wear by performing runs in an oxidising (air) atmosphere and comparing it to runs performed in an inert (nitrogen) atmosphere over a range of temperatures for filtered and unfiltered fuel oil samples. The oxidation products form an oxide film on the contacting surfaces which tends to slow down or arrest oxidation.

Friction and wear tests were performed for both filtered and unfiltered fuel oils, containing different asphaltene content, at different temperatures under oxidising (air) and inert (nitrogen) atmosphere using a HFRR lubricity tester according to the ISO 12156-1 standard. Three fuel oil samples with unique characteristics were used, namely a light cycle oil (LFO), a medium wax-blend oil (MFO) and a crude-derived heavy fuel oil (HFO).

2. Literature review

2.1 Introduction

Fuel oil combustion is responsible for a significant portion of the energy demand for electricity generation (Elbaz *et al,* 2018). The characteristics of fuel oil combustion are crucial for power plant equipment such as furnaces, gas turbines and boilers (Elbaz *et al,* 2018). Fuel oils are passed through pumps, filters, nozzles and other equipment which require good lubricating properties before they reach the burner section. Pumps which require a lubricating film between moving surfaces are vulnerable to premature wear, high repair and maintenance costs and potential failure of pumps when handling poor-lubricating liquids such as thin distillates (Nickels, 2011). Pumps used for handling heavier oils rely on a full film of oil to prevent metal contact and wear as the motors turn, impellers rotate and as parts of the pump rotate, reciprocate or move. Film failure impairs the movement between the contacting surfaces and causes severe wear which damages the contacting surfaces (Stachowiak & Batchelor, 2014: 5).

2.2 Friction

Friction is the resistance to motion that is experienced when one body moves tangentially whilst in contact with another body (Bhushan, 2013: 199). Friction is categorised as internal or external friction. External friction, which consists of dynamic and static friction, is the force which hinders or resists movement between sliding surfaces. Asperities are microscopic contact points between two sliding surfaces that cause external friction. These contact points cause adhesive wear, surface deformation and grooving. The energy loss through friction can be measured as heat and as mechanical vibrations. Lubricants can reduce or avoid surface contact causing external friction. Internal friction results from the friction between lubricant molecules, which is measured by the lubricant's viscosity (Mang & Dresel, 2017: 13). The viscosity of lubricating oils decreases as the temperature increases. An increase in temperature reduces the cohesion forces between the molecules of the oil and hence decreases the viscosity (Mang & Dresel, 2017: 33).

Coefficient of friction (a dimensionless value) is the ratio of the frictional force F to the normal force N (Bhushan, 2013: 201; Mang & Dresel, 2017: 14).

$$\mu = \frac{F}{N} \tag{1}$$

Frictional force is the force resisting the relative motion which acts in the opposite direction of the motion. According Bharat Bhushan, “The friction force (or coefficient of friction) is independent of the apparent area of contact between the contacting bodies. Thus two bodies, regardless of their physical size, have the same coefficient of friction” (Bhushan, 2013: 201). High friction occurs if both contacting surfaces are without chemical films and adsorbed substances. A high coefficient of friction indicates poor lubrication with significant metal-to-metal contact taking place in the boundary lubrication regime resulting in wear (PCS Instruments, 2005). Friction is undesirable in most sliding and rotating components such as seals and bearings. In the cases where friction is undesirable, friction is minimized because it causes energy loss and wear of contact surfaces (Bhushan, 2013: 199).

2.3 Wear

Wear is the progress of the removal of material from the surface to a another contacting surface due to mechanical processes (Mang & Dresel, 2017: 21). According to Zenon Pawlak, “Wear occurs when the shear strain reaches a certain critical value of the coefficient of friction, resulting in surface disruption and wear” (Pawlak, 2003: 165). The mechanical causes of wear are the contact and the relative movement of a contacting solid or liquid to the body (Mang & Dresel, 2017: 21). Wear causes loss of material and damage from one or both solid surfaces in a sliding motion relative to one another (Bhushan, 2013: 315). Wear is created by the processes of adhesion, abrasion, tribochemical reactions, erosion and metal fatigue and can occur chemically or mechanically. Frictional heat and temperature typically accelerate wear (Mang & Dresel, 2017: 21; Bhushan, 2013: 316).

In most cases, wear occurs through surface interactions at asperities (Bhushan, 2013: 315). Surfaces on the microscopic scale are rough, although they may appear smooth. When pressure is placed on two surfaces, the asperity peaks make contact. As a result, the real contact area is much less than the apparent contact area (Mang &

Dresel, 2017: 904). Wear can be measured by weight, volume or area (Mang & Dresel, 2017: 25). Wear volume V is described by Equation 2 (Pawlak, 2003: 165; Kauzlarich & Williams, 2001)

$$V = K_w W L \tag{2}$$

where K_w is the dimensional wear coefficient constant which is experimentally determined in $mm^3(Nm)^{-1}$, W is the load in N and L is the sliding distance in m. In situations of very mild wear the K_w value is less than 10^{-9} $mm^3(Nm)^{-1}$ while in situations of severe wear the K_w has values of 10^{-4} or more (Kauzlarich & Williams, 2001).

Wear includes abrasive, adhesive, chemical (corrosive), fatigue, impact by erosion and percussion, and electrical-arc-induced wear. These different wear phenomena all remove solid material from rubbing surfaces (Bhushan, 2013: 316). Adhesive wear and abrasive wear are the most important mechanical wear (Pawlak, 2003: 165).

2.3.1 Adhesive wear

Adhesive wear is a phenomenon where high unstable coefficient of friction and high wear rates occurs. Adhesive wear results in most lubricant failures since adhesive wear is associated with failure of the lubricant to provide some separation between the sliding surfaces (Stachowiak & Batchelor, 2014: 577). Adhesion occurs at the asperity contacts, these asperity contacts are sheared by sliding, which results in detachment of material from one surface and attachment of material to the other surface (Bhushan, 2013: 316). The greatest adhesion occurs for a combination of like materials such as iron to iron adhesion. In material combinations with dissimilar metals, when there is strong adhesion, wear particles of both metals are formed where larger and more transfer of the weaker metal to the stronger metal occurs (Stachowiak & Batchelor, 2014: 577; Bhushan, 2013: 318). Increase in surface hardness or roughness of contacting surfaces results in reduced adhesion (Stachowiak & Batchelor, 2014: 577). Figure 1 shows the process of metal transfer between a weak and strong material due to adhesion.

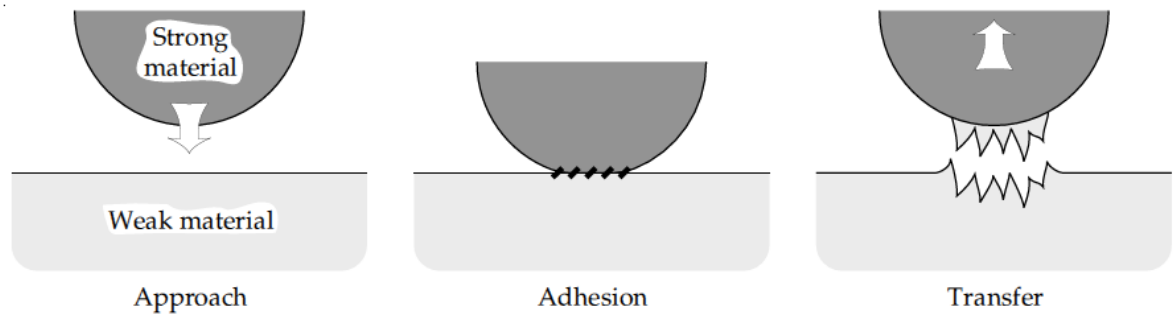

Figure 1: Process of metal transfer due to adhesion (Stachowiak & Batchelor, 2014: 578).

Surface tension is the work required to pull apart a solid resulting in a new surface being generated. This is associated with adhesive behaviour of solids in solid-state contact (Pawlak, 2003: 167).

Adhesion is considered to be either chemical or physical. Chemical adhesion interaction involves the covalent, ionic, electrostatic and metallic bonds (intramolecular forces) while physical adhesion interaction involves hydrogen bonds and van der Waals forces (intermolecular forces). The intermolecular forces are much weaker than the intramolecular forces because there is no electron exchange (Stachowiak & Batchelor, 2014: 581). Adhesion between a metal surface (e.g tungsten) and polymers (e.g polytetrafluoroethylene or polyimide) cause polymers to transfer to the metallic surface when the two materials are separated. Most polymers adhere to other materials by physical adhesion (van der Waals forces). In most cases, physical adhesion is not strong enough for detachment of material because the van der Waals forces are weak forces (Stachowiak & Batchelor, 2014: 580).

2.3.2 Abrasive wear

Abrasive wear occurs when a hard surface with asperities or hard particles slide on a softer surface resulting in plastic deformation or fracture of the interface. In many cases, adhesive wear is the wear mechanism at the start of abrasive wear which form wear particles that get caught at the interface, resulting in three body abrasive wear (Bhushan, 2013: 328). The third body in three body abrasion is generally small particles of abrasive material trapped between the two surfaces and able to abrade

one or two surfaces because the particles are sufficiently harder (Bhushan, 2013: 329).

The modes of deformation of abrasive wear are ploughing, wedge formation and cutting (Bhushan, 2013: 330). According to Bharat Bhushan, "The controlling factors for the three modes of deformation are the attack angle or degree of penetration, and the interfacial shear strength of the interface" (Bhushan, 2013: 331). Figure 2 and Figure 3 show the schematic and SEM micrographs for the modes of deformation of abrasive wear respectively.

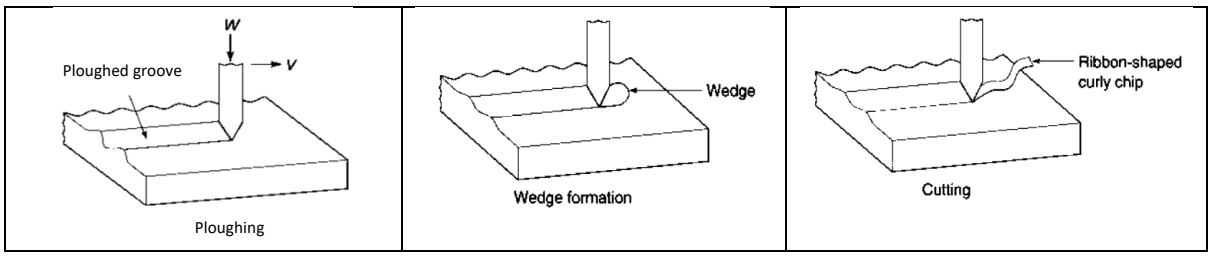

Figure 2: Schematic of the modes of deformation of abrasive wear (Bhushan, 2013: 331)

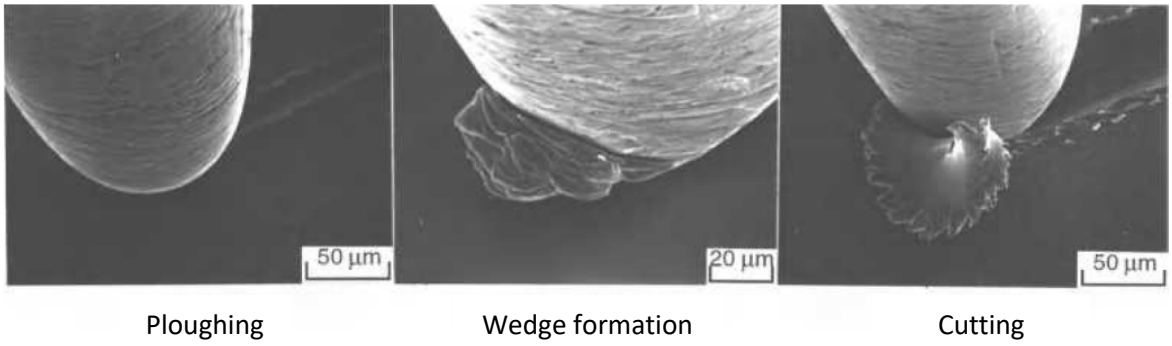

Figure 3: SEM micrographs of the modes of deformation of abrasive wear (Bhushan, 2013: 332).

2.3.3 Chemical wear

The removal of chemically reacted surface layers by friction processes is called chemical wear (Mang & Dresel, 2017: 24). Chemical wear occurs when sliding takes place in corrosive, high temperature and high humidity environments. Oxidative wear is chemical wear that is due to atmospheric oxygen being the corroding agent (Bhushan, 2013: 359). Air is the most corrosive medium due to the presence of oxygen

(Mang & Dresel, 2017: 24). Oxides, the chemical products of chemical wear, form a film (<1 nm thick) on the surfaces in the absence of sliding. The oxides tend to slow down or arrest oxidation. The sliding motion wears the oxides away allowing the chemical attack to continue. Thus chemical wear requires both chemical reaction and rubbing (Bhushan, 2013: 359). Figure 4 shows a bearing after chemical wear.

Figure 4: SEM micrograph of a hardened roller bearing after chemical wear (Bhushan, 2013: 360).

Tribochemical wear is the phenomenon by which friction increases the chemical reaction rate as frictional heat is produced at contacting asperities (Pawlak, 2003: 170). Chemical reactions can be accelerated by supplying energy thermally and mechanically. Chemical reactions can also increase due to the removal of chemical films or reaction products resulting in fresh surfaces, direct mechanochemical excitation of surface bonds and accelerated diffusion (Bhushan, 2013: 361; Adams *et al*, 2015).

2.4 Lubrication

Lubrication is related to diagnosing and improving the effectiveness of films in preventing damage of solid contacts (Stachowiak & Batchelor, 2014: 3). A mechanical lubrication system has three components that must be considered: the effectiveness of the lubricant, the metal surface to be lubricated and the environment (Pawlak, 2003: 161). Films are the thin low shear strength layers of liquid that is between two surfaces. These films are hard to detect and often range from 1-100 µm. Films separate contacting bodies, reduces roughness of the moving surfaces and prevent damage

(Stachowiak & Batchelor, 2014: 3). A thin film between moving surfaces, results in lower friction and wear, as compared to metal-to-metal contact. A thick fluid between moving surfaces prevents metal-to-metal contact and results in extremely low friction (0.001-0.003) and negligible wear. Polar compounds containing oxygen, nitrogen, aromatics and olefinic contents are responsible for lubricity of fuels because they are adsorbed on the rubbed metal surfaces providing a protective layer that limits friction and wear (Lapuerta *et al*, 2016; Agarwal *et al*, 2013).

2.4.1 Lubrication regimes

There are four liquid lubricating regimes namely: hydrodynamic, elastohydrodynamic, mixed and boundary regime. These regimes are dependent on oil viscosity, relative velocity and are inversely proportional to the load (Pawlak, 2003: 168). The Stribeck curve in Figure 5 shows the coefficient of friction plotted against the dimensionless parameter called the Hersey number. The Hersey number is obtained from the velocity times the dynamic viscosity divided by the load per unit length (Shaffer, 2014). The lubricant's film thickness h is dependent on the lubrication conditions, including the surface roughness R and friction (Mang & Dresel, 2017, 18).

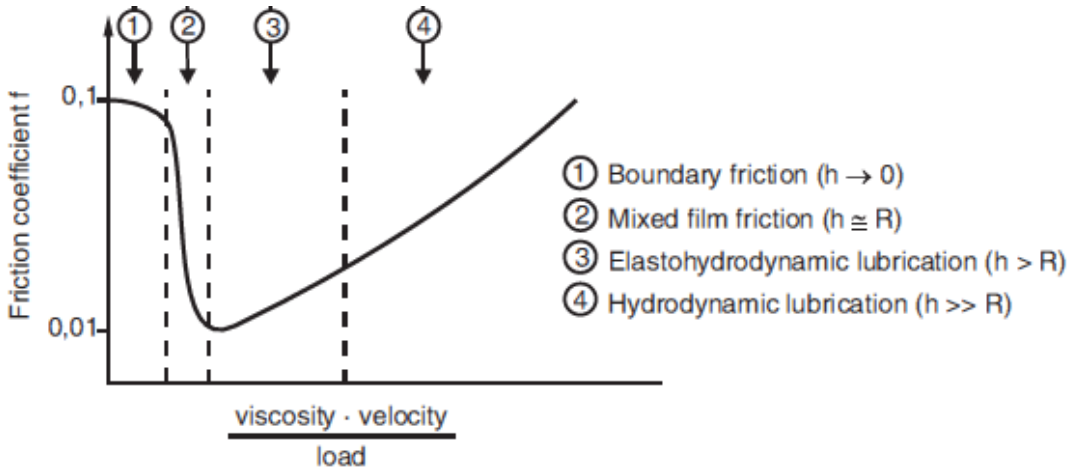

Figure 5: Stribeck curve (Mang & Dresel, 2017: 18).

2.4.1.1 Hydrodynamic lubrication

Hydrodynamic lubrication is characterised by complete separation of the surfaces by a fluid film. The fluid film is developed by the flow of fluid on the interface (Pawlak, 2003). Hydrodynamic lubrication which is an ideal lubrication regime because the fluid

films are generally much thicker than the height of surface asperities. Thus, solid contacts does not occur resulting in negligible deformation (Bhushan, 2013: 401; Pawlak, 2003: 168). Hydrodynamic lubrication results in separation of the contacting surfaces which prevent mechanical wear from solid-solid contact and abrasion (Pawlak, 2003: 168).

2.4.1.2 Elastohydrodynamic lubrication

Elastohydrodynamic lubrication is a unique form of hydrodynamic lubrication involving interaction between the contacting surfaces and the liquid lubricant (Stachowiak & Batchelor, 2014: 4). The elastohydrodynamic regime is characterised by continuous fluid film and elastic deformation (Bhushan, 2013: 402). Elastic deformation of the contacting surfaces is caused by the high loads because the speed and viscosity are low enough to not produce a thick film (Pawlak, 2003: 168). The film thickness in elastohydrodynamic lubrication is thinner than that in conventional hydrodynamic lubrication and the elastohydrodynamic film supports the load (Bhushan, 2013: 402).

2.4.1.3 Boundary lubrication

In the boundary regime, contact of asperities occurs between the moving surfaces, and the chemical compounds are sheared. The boundary regime is characterised by contact, elastic and plastic deformation (Pawlak, 2003: 168). Surface contact of asperities occurs frequently with a significant energy dissipation (Pawlak, 2003: 164). Boundary lubrication involves chemical interactions between contacting surfaces and the liquid lubricant. The surface interaction between the films and asperities is prominent because the contacting surfaces are close together (Bhushan, 2013: 403). These contact interactions produce elastic and plastic deformation, friction, heat and sometimes wear (Pawlak, 2003).

Boundary lubrication usually occurs under extreme pressure conditions such as high load, low velocity conditions. The viscosity of the lubricant is of minor importance in boundary lubrication. Failure in the boundary regime happens due to adhesive wear and corrosive wear (Bhushan, 2013: 403). The wear of the surfaces and the friction is much higher when compared with elastohydrodynamic lubrication (Pawlak, 2003: 165). Boundary lubrication also results via the metal-to-metal interactions between the impurities in the lubricant and the solid surfaces. These impurities such as aromatics,

sulphur and nitrogen compounds are adsorbed or react on rubbed metal surfaces to limit adhesion, wear, friction and seizure (Agarwal *et al*, 2013).

2.4.1.4 Mixed lubrication

The transition between the hydrodynamic/elastohydrodynamic regime and boundary regime is known as the mixed lubrication regime in which both lubrication regimes may be operating. The mixed lubrication regime is also often referred to as partly hydrodynamic, partial fluid or thin film lubrication (Bhushan, 2013: 403).

2.4.2 Adsorption

2.4.2.1 Physical adsorption

Physical adsorption is a physical mechanism where molecules are attracted to a surface by van der Waals forces. Adsorption is temperature-dependent and drastically reduces at high temperatures. At temperatures above 200 °C, the adsorption of molecules is most likely to be ineffective. Adsorption increases with increasing pressure. The adsorption of molecules is influenced by the polar groups, more polar molecules are more strongly adsorbed compared to less polar molecules. More polar molecules result in an increase in its concentration on the metal surface resulting in reduction of the friction coefficient (Pawlak, 2003: 161). Physical adsorption on metal surfaces provides surface protection against the deposition of pollutants (Pawlak, 2003: 15). Polar groups are adsorbed on metal surfaces which provides protection of the metal surface from corrosion (Pawlak, 2003: 24).

2.4.2.2 Chemisorption

Chemisorption is a phenomenon that involves the interaction of strong chemical bonds between the liquid and the solid surface. According to Zenon Pawlak, “Chemisorption is a monolayer process, where exchange of orbital electrons occurs between adsorbed molecules and atoms of the surface, causing the formation of new chemical compounds” (Pawlak, 2003: 163). Chemisorbed molecules are stronger than physically adsorbed molecules, and therefore have a greater resistance to high temperatures, and mechanical shear (Pawlak, 2003: 163).

2.5 Fuel oils

There are two basic types of fuel oil: distillate fuel oil and residual fuel oil. Fuel oils comprise of a range of liquid combustibles, mainly hydrocarbons, which were obtained either as distillates in the working up of petroleum or as residues after the lighter fractions have been removed (Harker & Allen, 1972: 120). Fuel oils are used for industrial and marine operations because fuel oils are cheaper than diesel (Elbaz *et al,* 2018). Distillate fuel oil is lighter, thinner and better for a cold start when compared to residual fuel oil (Martinez, 2018). Distillate fuel oil and residual fuel oil are often blended together to get a fuel oil with a required (lower) viscosity than that of the residual fuel oil (Elbaz *et al,* 2018).

2.5.1 Fuel oil Refining Process

Crude oil is, an extremely complex mixture of hydrocarbons, used as a raw material for the petrochemical plant to produce fuels, synthetic rubber, plastics and additional products (Elbaz *et al,* 2018). The oil refining process separates the extremely complex mixture of hydrocarbons in crude oil by their differences in boiling point by distillation. Numerous products are produced by distillation of crude oil such as petrol (gasoline), fuel oils, jet fuel and other products. These products contain mostly hydrocarbons with other elements such as sulphur, nitrogen and oxygen being present in the petroleum products. The heavier products may contain a few metals and salts. In a refinery, the valuable products that are produced can be maximized by including other processes that break down the long-chains into shorter chains, remove impurities and combine mixtures of different hydrocarbons to produce the required products. These processes breakdown the distilled bottom fraction, the heaviest products with the highest boiling points, into lighter products. Some processes that convert long chains to shorter chains are thermal cracking, catalytic cracking, and hydrocracking (Litzke, 2004).

The various kinds of fuel oils are obtained by the distillation of crude oil. The most volatile fractions are removed first, which are naptha and benzene. After removing these volatile fractions the first fuel oil which is distilled is called Kerosene. The distilled bottom fraction is very viscous being comprised mostly of the heavy long-chain hydrocarbons. This fraction is called the residual fuel oil (Elbaz *et al,* 2018). Figure 6 shows a typical oil refining process beginning with the feedstock crude oil.

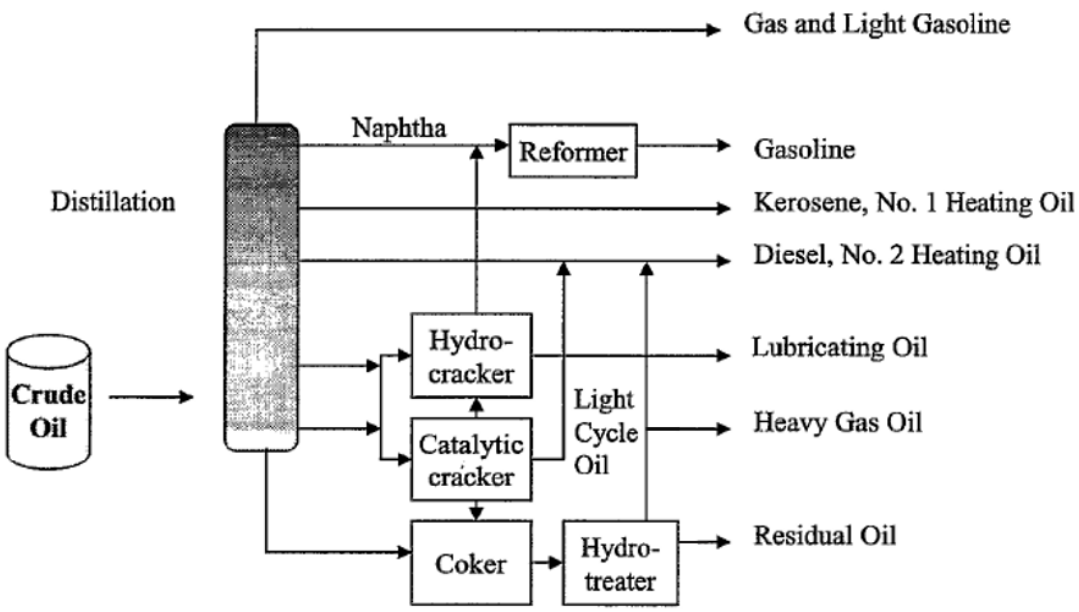

Figure 6: Oil refinery process of crude oil (Litzke, 2004).

2.5.2 Fuel oil specifications

Fuel oils consist of a complex mixture of aliphatic and aromatic hydrocarbons. Fuel oils comprise of 80-90% of aliphatic alkenes (paraffins) and cycloalkanes (napthenes) which are hydrogen saturated, 10-20% aromatics and 1% olefins (ATSDR, 2014). The ASTM D396 standard covers grades of fuel oil intended for use in fuel oil burning equipment. The standard classifies fuel oils into six grades numbered in order of increasing density and viscosity, with number six being the heaviest fuel oil and number one being the lightest fuel oil (Litzke, 2004). The fuel oils labelled no.1, 2 and 3 are referred to as distillate fuels oils while no.4, 5 and 6 are referred to as residual fuel oils (Srivastava & Hancsók, 2014: 336). Table 1 shows the fuel oil specifications according to ASTM D396.

Table 1: Requirements for fuel oils (ASTM D396-18a, 2018)

Property	**No. 1** 1. S15, 2. S500, 3. S5000	**No. 2** 1. S15, 2. S500, 3. S5000	**B6-20** 1. S15, 2. S500, 3. S5000	**No. 4** 1. Light, 2. No 4	**No. 5** 1.Light, 2. Heavy	**No. 6**
Flashpoint, °C, min	38	38	38	1)38, 2)55	55	60
Water and sediment, volume %, max	0.05	0.05	0.05	1)0.05, 2)0.5	0.5	0.5
Distillation Temperature, °C 10% VR, max 90% VR, min 90% VR, max	 215 - 288	 - 282 338	 - 282 343			
Kinematic viscosity (40 °C), $mm^2(s)^{-1}$ Min Max	 1.3 2.4	 1.9 4.1	 1.3 4.1	 1)1.9, 2)>5.5 1)5.5, 2)24	 -	 -
Kinematic viscosity(100 °C) , $mm^2(s)^{-1}$ Min Max	 - -	 - -	 - -	 - -	 1)5.0, 2)9.0 1)8.9, 2)14.9	 15 50
Ramsbottom carbon residue on 10% distillation residue mass %, max	0.15	0.35	0.35	-	-	-
Ash, mass%, max	-	-	-	1)0.05, 2)0.10	0.15	-
Sulphur, mass%, max	1) 0.0015 2) 0.05 3) 0.5	1) 0.0015 2) 0.05 3) 0.5	1) 0.0015 2) 0.05 3) 0.5			
Lubricity, HFRR @60 °C, micron, max	520	520	520			
Copper strip corrosion rating, max,	No 3	No 3	No 3	-	-	-
Density at 15 °C, $kg(m)^{-3}$, min Max	- 850	- 876	- 876	1)>876, 2)- -	- -	- -
Pour Point, °C, max	-18	-6	-6	-6	-	
Oxidation stability, hours, min	-	-	6			
Acid number, mg $KOH(g)^{-1}$, max	-	-	0.3			
Biodiesel content, % (v/v)	-	-	6-20	-		
Conductivity $\rho S(m)^{-1}$, min	25	25	25			

The **flashpoint** of a liquid fuel is the temperature at which the fuel begins to release enough vapours to form an explosive or flammable mixture in air. The flashpoint is an indirect measure of volatility and an indication of the fire hazards associated with the application and storage of the fuel (Harker & Allen, 1972: 101). Generally flashpoint is important for fuel oils since it refers to a temperature above normal or ambient temperature (Harker & Allen, 1972: 102). Regulations governing the safety aspects of fuel storage dictate that the flash-point of fuel oil should not be lower than 339 K (65.85 °C) (Harker & Allen, 1972: 101).

Flash point can be determined by open or closed flash point method. Closed indicates that the vapour and air mixture is in a confined space above the liquid. Two types of apparatus are used to determine the closed flash point of a fuel. The Pensky Martin apparatus is used for flash point above 322 K while the Abel apparatus is used for flash point lower than 322 K. Each apparatus operates on the same principles. The oil under test is heated at a constant rate in a covered metal cup. A small test flame is introduced at intervals through an opening in the lid of the cup. The temperature at which insertion of the flame causes vapour-air-mixture above the oil in the cup to ignite is the flash point (Harker & Allen, 1972: 101). For the open flash point method, a flash point is determined when liquid fuel is heated in an open crucible and the test flame is repeatedly applied above the surface. This is usually several degrees higher than the corresponding closed flash point, since its ignition takes place when there is just sufficient vapour in excess air rather than in a restricted space as with the closed flash point. The open flash point has the disadvantage that traces of very volatile material may be lost in air across the surface. A fresh sample of oil must be used to check a flashpoint value as volatiles are lost from the mixture during a determination (Harker & Allen, 1972: 102).

2.5.2.1 Distillate fuel oil

Straight run kerosene is a light distillate fuel oil, without further processing, which consists primarily of hydrocarbons in the C_{11}-C_{20} range (Litzke, 2004). Kerosene is intended for use in vaporising type burners due to its high volatility. High volatility of fuel oil is necessary for vaporising type burners to ensure that evaporation continues

with minimal residue. Kerosene is converted to vapour by heating the kerosene or by radiation (Curl & O'Donnell, 1977).

Fluid catalytic cracking reactor units in the refinery convert heavy fuel oils into lighter products. Light cycle oil (LCO) is a by-product of the fluidized catalytic cracking reactor. LCO can be used as a blending component in heavy fuel oils for viscosity adjustments in order to reduce the final viscosity. The distillation and viscosity characteristics of LCO are similar to diesel fuel. LCO has high aromatic content (around 80 wt %) and high sulphur content (0.2-2.5 wt %) compared to diesel fuel, therefore LCO is considered as low-grade fuel and a poor blending component for diesel fuel (Pasadakis *et al*, 2011; Cao *et al*, 2021).

Diesel fuel oil (No. 2 heating oil) is generally a blend of straight-run product, LCO and hydrocracked products. Diesel fuel oil, a heavier distillate fuel oil than kerosene, contains approximately 64% aliphatic hydrocarbons, 35% aromatic hydrocarbons and 1-2% olefinic hydrocarbons (ATSDR, 2014). Diesel fuel oil, used in commercial-industrial burners and in domestic burners, is created for atomizing type burners. The diesel fuel oil is sprayed into a combustion chamber where tiny droplets burn while in suspension (Curl & O'Donnell, 1977). Diesel fuel oil has a higher cost compared with residual fuel oil because diesel fuel oil is easier to handle and readily available. The distinction between diesel fuel used for vehicles and heating fuel oil is its sulphur content. Diesel for vehicles, defined as low sulphur, must have sulphur content at or below 10 ppm per SANS 342 and have a cetane number higher than diesel fuel oil (No. 2 heating oil), a key characteristic for diesel engines, which affects how smoothly the fuel burns, however, it is irrelevant for heating fuel oils (Litzke, 2004; SANS 342, 2016).

2.5.2.2 Residual fuel oil

Residual fuel oil is the residue of crude oil distillate that is still flowable under standard temperature and pressure (25 °C and 101.325 kPa). The semi-solid residue of the crude oil distillate is called asphalt (Martinez, 2018). Waste oils from other industries are often added to residual fuel oils. Residual fuel oil is used in large marine vessels because of its low cost compared to other fuel oils. The price of residual fuel oils is much lower than distillate fuel oils. A distinct composition cannot be determined for

residual fuel oils, because of their complexity and variability. Residual fuel oils have complex composition and impurities compared distillate fuel oils (ATSDR, 2014; Elbaz *et al,* 2018).

2.5.3 Marine fuel specifications

The fuel testing of marine fuel oils ensures that the fuel oils are within the required specifications under the ISO 8217 standard. The ISO 8217 standard specifies the requirements for the fuel oils which are used in marine diesel engines and boilers prior to conventional on board treatment before use. The residual marine fuel oils containing water, sediments and catalyst fines are supplied to marine ships. These impurities must be removed on board before using the fuel oils (Srivastava & Hancsók, 2014). The on board treatments are settling, centrifuging and filtration. The ISO 8217 standard looks at the following specifications: viscosity, density, water, calculated carbon aromaticity index (CCAI), compatibility, pour point, salt content and sulphur content. Table 2 and Table 3 shows the requirements for marine distillate fuel oils and marine residual fuel oils respectively.

The distillate marine fuel oils consists of three distillate fatty acid methyl esters (DF) grades and four distillate marine (DM) grades. The DF grades DFA, DFZ and DFB include up to 7 volume % fatty acid methyl esters (FAME). The DM grades are named DMA, DMZ, DMB and DMX. Other than the FAME allowance, the DFA, DFZ and DFB grades are identical to the DM grades DMA, DMZ and DMB respectively. DMA, DMZ, DMB and the six residual marine (RM) grades named RMA, RMB, RMD, RME, RMG, RMK have minimal FAME levels while DMX must be FAME free (ISO 8217, 2017)

Table 2: Distillate marine fuel oils (ISO 8217, 2017).

Property		Limit	Category ISO-F						
			DMX	DMA	DFA	DMZ	DFZ	DMB	DFB
Kinematic viscosity (40 °C), cSt		Max	5.5	6		6		11	
		Min	1.4	2		3		2	
Density (15 °C), kg(m)$^{-3}$		Max	–	890		890		900	
Cetane index		Min	45	40		40		900	
Sulphur, mass%		Max	1	1		1		35	
Flash point, °C		Min	43	60		60		1.5	
Hydrogen sulfide, mg(kg)$^{-1}$		Max	2	2		2		60	
Acid number, mg KOH(g)$^{-1}$		Max	0.5	0.5		0.5		2	
Total sediment by hot filtration, mass%		Max	–	–		–		0.5	
Oxidation stability, volume%		Max	25	25		25		25	
Fatty acid methyl ester, mass%		Max	–	–	7	–	70	–	70
Carbon residue (10% v), mass%		Max	0.3	0.3		0.3		–	
Carbon residue, Mass%		Max	–	–		–		0.3	
Cloud point, °C	Winter	Max	-16	Report		Report		–	
	Summer	Max	-16	–		–		–	
Cold filter plugging point, °C	Winter	Max	–	Report		Report		–	
	Summer	Max	–	–		–		–	
Pour point (upper), °C	Winter	Max	–	-6		-6		0	
	Summer	Max	–						
Appearance			Clear and bright						
Water, volume%		Max	–	–		–		0.3	
Ash, mass%		Max	0.01	0.01		0.01		0.01	
Lubricity, corrected WSD at 60 °C, µm		Max	520	520		520		520	

Table 3: Residual marine fuel oils (ISO 8217, 2017).

Property		Limit	Category ISO-F-					
			RMA	RMB	RMD	RME	RMG	RMK
			10	30	80	180	**1.** 180 **2.** 380 **3.** 500 **4.** 700	**1.** 380 **2.** 500 **3.** 700
Kinematic viscosity at 50 °C, cSt		Max	10	30	80	180	**1.** 180 **2.** 380 **3.** 500 **4.** 700	**1.** 380 **2.** 500 **3.** 700
Density at 15 °C, $kg(m)^{-3}$		Max	920	960	975	991	991	1010
CCAI		Max	850	860	860	860	870	870
Sulphur, mass%		Max	Statutory requirements					
Flash point, °C		Min	60	60	60	60	60	60
Hydrogen sulphide, $mg(kg)^{-1}$		Max	2	2	2	2	2	2
Acid number, mg $KOH(g)^{-1}$		Max	2.5	2.5	2.5	2.5	2.5	2.5
Total sediment-Aged, mass%		Max	0.1	0.1	0.1	0.1	0.1	0.1
Carbon residue, mass%		Max	2.5	10	14	15	18	20
Pour point, °C	Winter	Max	0	0	30	30	30	30
	Summer	Max	6	6	30	30	30	30
Water, volume%		Max	0.3	0.5	0.5	0.5	0.5	0.5
Ash, mass%		Max	0.04	0.07	0.07	0.07	0.1	0.1
Vanadium, $mg(kg)^{-1}$		Max	50	150	150	150	350	450
Sodium, $mg(kg)^{-1}$		Max	50	100	100	50	100	100
Aluminium plus silicon, $mg(kg)^{-1}$		Max	25	40	40	50	60	60
Used lubricating oil: Calcium and zinc/phosphorus, $mg(kg)^{-1}$			Calcium >30 and zinc >15 or Calcium >30 and phosphorus >15					

The **cloud point** is the temperature at which oil begins to cloud due to the separation of wax on cooling. The **pour point** of oil is the lowest temperature at which the oil will

flow, or pour, when cooled without agitation under standard conditions (Harker & Allen, 1972: 108). The **cold filter plugging point** of oil is the temperature at which a test filter becomes clogged by wax as the fuel is cooled (Litzke, 2004).The pour point, cloud point and cold filter plugging point are important characteristics for distillate marine fuel oils because issues with low temperature operability can occur in distillate fuel oils. These could be the deposition of solidified wax in the fuel tanks, fuel lines, centrifuges and filters (ISO 8217, 2017).

The CCAI is specified for the residual fuel oils in Table 3. The CCAI (a dimensionless value) is calculated by using Equation 3 (ISO 8217, 2017)

$$CCAI = \rho_{15} - 81 - 141.log[log(\text{kv} + 0.85)] - 483.log\left[\frac{T + 273}{323}\right] \qquad (3)$$

where ρ_{15} is the density at 15 °C and the kv is the kinematic viscosity in $mm^2(s)^{-1}$ at temperature T in °C.

The specifications that are important to ensure reliable engine operation with residual fuel oils are the density limit, alumininium limit, silicon limit and the total sediment age limit which are shown in Table 3. The maximum density limit in residual fuel oils is important for purifier operation and for satisfactory ignition quality for low viscosity fuel oil grades. The maximum aluminium and silicon limit is important in order to avoid abrasive wear damage in the fuel system on board. The aluminium and silicon should be sufficiently removed by the ship's fuel cleaning system because aluminium silicate catalyst particles are not completely removed from the residual fuel oil. The maximum total sediment (aged) limit is important because the stability of the asphaltenes is deteriotated by the visbreaking process shown in Figure 7 and instability problems of the asphaltenes can cause filter-blocking and fuel purification problems, and therefore the requirement for a specification to ensure adequate fuel stability (Vermeire, 2012).

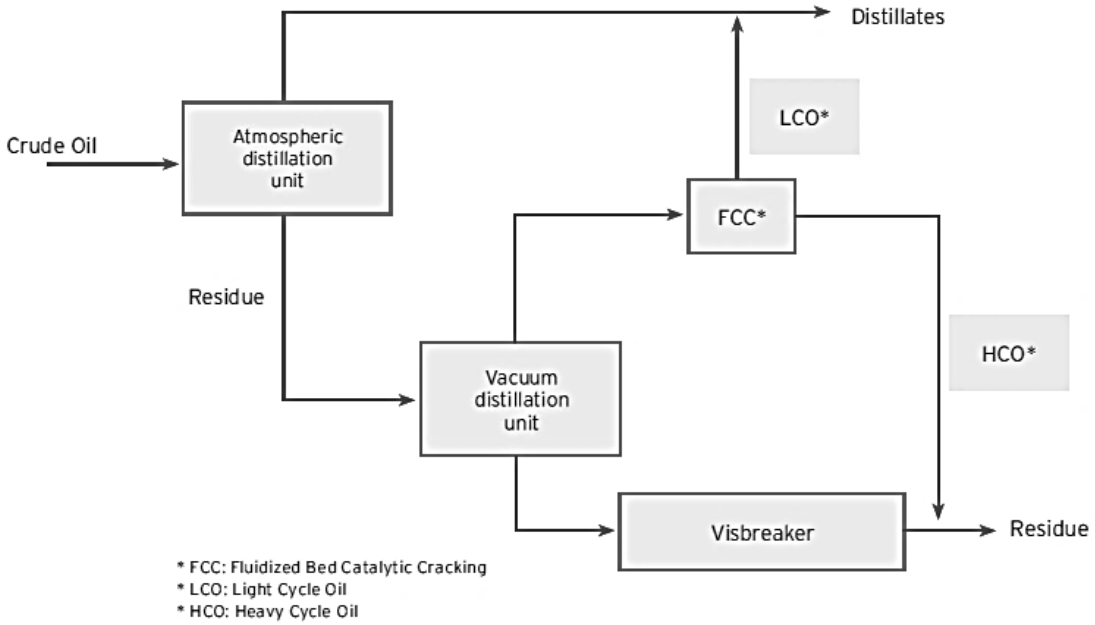

Figure 7: Complex refinery with fluid catalytic cracking and visbreaking (Vermeire, 2012).

2.5.4 Properties affecting performance/behaviour/utilisation of fuel oils

The improvement of fuel oil reliability and minimizing service costs associated with fuel oil performance is of top priority in the fuel oil industry (Litzke, 2004). Fuel oil is difficult to handle because it must be settled, preheated and filtered before being used (Elbaz *et al,* 2018). Burner shut-downs can be caused by contamination of fuel, fuel degradation and poor fuel quality. Fuel stability, thermal stability, viscosity and fuel cleanliness affect the fuel flow and the nozzle and filter clogging tendencies of fuel (Litzke, 2004).

2.5.4.1 Fuel Stability

The stability and ease of processing of fuel oil depends on the crude oil sources from which the fuel oil was derived, the use of additives and other refinery processes. Fuel oils produced from different refineries may vary in composition and stability properties (Litzke, 2004).

2.5.4.2 Thermal stability

Thermal stability is the lubricant's ability to resist degradation or cracking due to heat. Thermal stability is important because it gives an indication of the highest temperature at which the lubricant can be used (Pawlak, 2003: 167). The products of thermal

decomposition may be corrosive and may, in addition, form a deposit (Pawlak, 2003: 21).

2.5.4.3 Particulate Matter

The formation of particulate matter introduces problems and expensive maintenance costs. The solid particles related with the heavy fuel oil's exhaust gases result in harmful effects on the environment and human health (Elbaz *et al,* 2018). The maximum particulate contamination in middle distillate fuel oils is 25 $(mg)m^{-3}$ by filtration according to the ASTM D6217-18 standard (ASTM D6217-18, 2018).

High sulphur content in heavy fuel oils affects the efficiency of the heating oil, fouling of boiler and fuel gas emissions by accelerating the formation of deposits and sediments in the heavy fuel oil and therefore increases the particulate matter and heavy metal impurities in heavy fuel oils (Litzke, 2004).

Slurries containing particles in the size range of microns causes clogging and choking of the system. Fluids with nanoparticles have a tendency for the nanoparticles to agglomerate, thus creating lumps, which reduce the fluid stability (Abdullah *et al*, 2018). Agglomeration of particles in the 1-5 micron range are enhanced by the level of impurities in the fuel (Kirk, 2015).

2.5.4.4 Asphaltenes

Asphaltenes are polar aromatic compounds with high molecular weight, which are partly dissolved and partly dispersed in crude oil (Ghanavati *et al*, 2013; Chandio *et al*, 2015). Asphaltenes are the heaviest fraction in crude oil and are formed by molecules containing aromatic rings, several heteroatomic and napthenic rings and relatively short paraffinic branches (Alcazar-Vara & Buenrostro-Gonzalez, 2011). Figure 8 shows the representative molecules of asphaltenes.

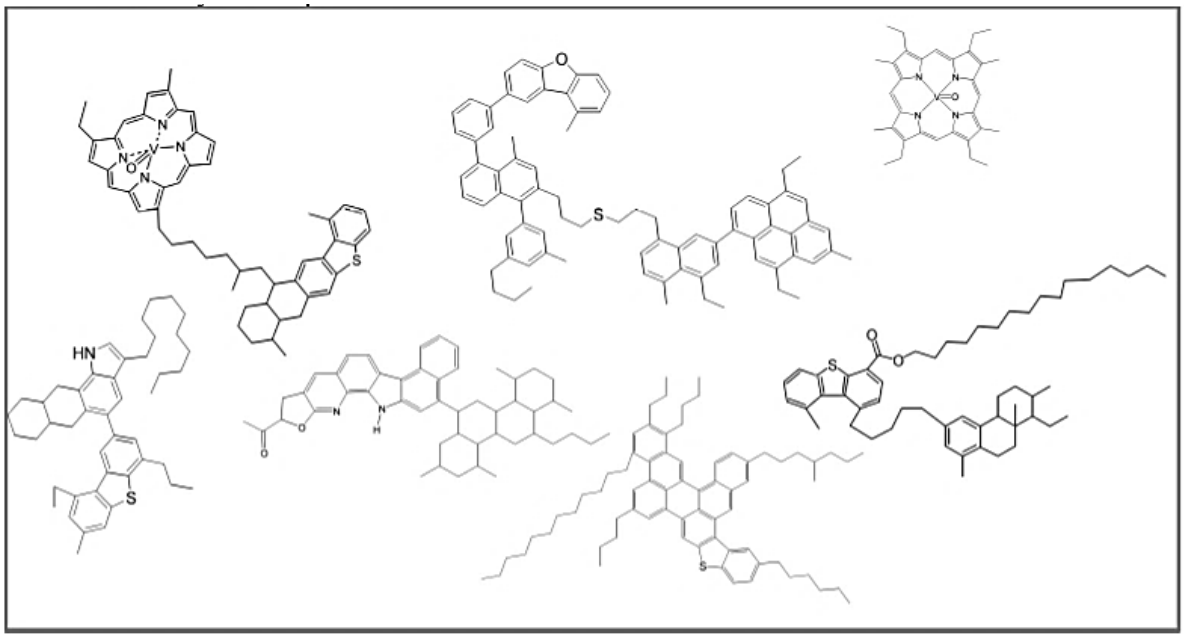

Figure 8: Representative asphaltene molecules (Ualbelta, sa).

Asphaltenes are not uniform in chemical composition as they are complex aromatic compounds with various carbonaceous sources containing around 40-50% aromatics. These aromatic molecules commonly contain heteroatoms (N, O, S) and metals (V, Fe, Ni etc) in the molecular structure (Zuo *et al*, 2019; Ghanavati *et al*, 2013). Asphaltenes have similar properties regardless of the source, molecular weight, composition and metal content (Zuo *et al*, 2019). In comparison to petroleum, asphaltenes have less hydrogen and more sulphur, nickel, vanadium and oxygen which results in a higher density (Ualbelta, *sa*).

Asphaltenes are major precursors of sludge or sediments and known to contribute to coke and sludge formation in refineries in addition to catalyst deactivation during processes (Garaniya *et al,* 2018; Ancheyta *et al*, 2009: 1). The asphaltenes fraction was initially separated from the heavy fuel oil because asphaltenes can cause unfavourable effects on the metal surface by becoming irreversibly adsorbed. In chromatography, asphaltenes are mostly removed from the sample before the analysis because asphaltenes contain very polar compounds which are likely to be irreversibly adsorbed by the adsorbent (e.g Silica, alumina) (Garaniya *et al,* 2018).

2.5.4.4.1 Properties

Asphaltenes are large molecules composed of numerous small molecules which form nanoaggregates. A key characteristic of asphaltenes is their ability to flocculate. Figure 9 shows dispersed asphaltene molecules that measure about 1.5 nm, nanoaggregates that measure about 2 nm and very high concentration asphaltene nanoaggregates which combine to form clusters that measure about 5 nm in heavy fuel oil (Mullins, 2016). A variety of analytical techniques shows that the mean aggregate size for asphaltenes range from 2-20 nm (Ualbelta, *sa*). There are two types of asphaltenes based on the size distribution of asphaltenes, dispersed asphaltenes (<2 μm) and aggregated asphaltenes (>2 μm) (Lei *et al*, 2016).

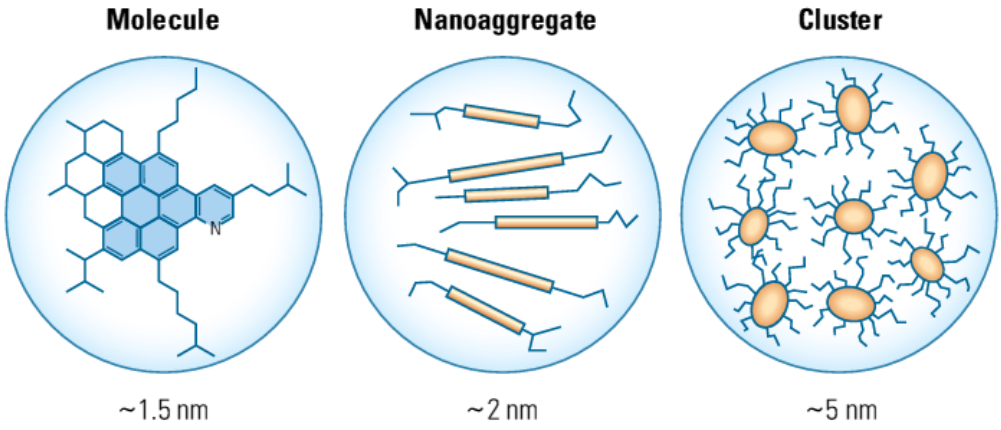

Figure 9: The Yen-Mullins model of asphaltenes (Mullins, 2016).

2.5.4.4.2 Solubility

Asphaltenes are not defined by their chemical identity, they are defined by their solubility characteristics because they consist of a complex mixture of compounds. This means that asphaltenes dissolve in light aromatic hydrocarbons and precipitate in low carbon number n-alkanes solvents (Ualbelta, *sa;* Garaniya *et al,* 2018). Asphaltene solubility follows the general rule in solution chemistry that “like” dissolves “like” and therefore dissolve in aromatic hydrocarbons (Mullins, 2016).

According to Hazlina Husin, “Asphaltenes deposition undergoes three stages: flocculation of small aggregates, precipitation of big aggregates and deposition of asphaltenes particles” (Husin *et al*, 2018). The effect of solvent carbon number on the solubility of asphaltenes shows that lower carbon number alkanes precipitate more

asphaltenes than higher carbon number alkanes (Yen & Chilingarian, 2000: 325). Figure 10 shows the amount of asphaltenes precipitated for different n-alkane solvents with various solvent-to-fuel oil ratio. The amount of precipitated asphaltenes decreases as the carbon number of n-alkanes increases (Ancheyta *et al,* 2009: 10).

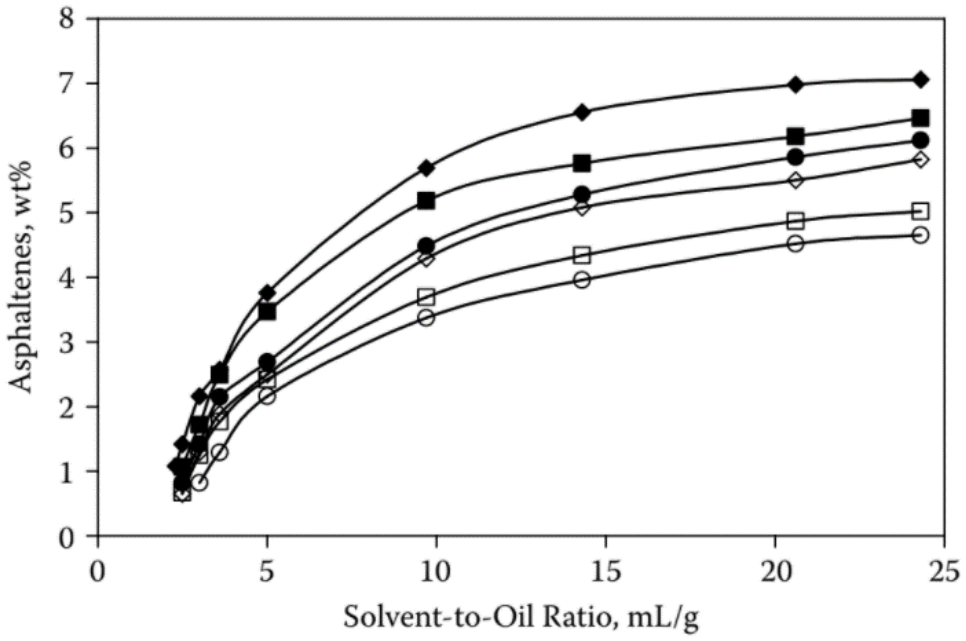

Figure 10: Amount of precipitated asphaltenes at 20°C using different n-alkane solvents: ((◆) C_5; (▲) C_6; (●) C_7, (◇) C_8, (□) C_9; (○) C_{10}) (Ancheyta et al, 2009: 11).

N-pentane results in larger yield of asphaltene precipitation when used as a solvent compared to when n-heptane is used. Lower alkane solvents precipitate a larger quantity of insoluble material because asphaltenes and resins are precipitated and, in some cases, some high molecular wax are precipitated (Ancheyta *et al*, 2009: 10; Garaniya *et al,* 2018). N-heptane is the solvent commonly used for asphaltenes precipitation from heavy fuel oils because their properties do not present major differences when using n-heptane or higher molecular weight alkanes (Ancheyta *et al*, 2009: 2). The remaining fractions, after the removal of asphaltenes, are known as maltenes which contain saturates, resins and aromatics. The low carbon n-alkanes precipitated asphaltenes are solid and powdery (Mullins, 2016). Asphaltene precipitation from the heavy fuel oil can be done according to the ASTM D2007 method (Ghanavati *et al*, 2013).

Asphaltenes precipitation and deposition occur during the operational process itself which means it is hardly avoidable (e.g. during the production of heavy fuel oil, lighter hydrocarbons or paraffinic oil are used as diluent to reduce the viscosity of crude oil). The use of lighter hydrocarbons or paraffinic oil can trigger asphaltene precipitation in tubings, pipelines and surface facilities (Husin *et al*, 2018). Fuel oils are said to be compatible when the mixing of two fuels does not cause asphaltenes coagulation. Two heavy fuel oils with different compositions can be incompatible with each other due to the different types of sources such as: the production of an atmospheric heavy fuel oil from a paraffinic crude oil, and the other heavy fuel oil from a visbreaker operation. Dispersants can be used to control the compatibility problem in heavy fuel oils (Srivastava & Hancsók, 2014: 347).

The characterisation of precipitated asphaltenes depend on the solvent power of alkanes in addition to other variables such as the alkane to fuel oil ratio, contact time and temperature (Rogel *et al*, 2016). The composition of precipitated asphaltenes also changes as a function of time (Rogel *et al*, 2016). The factors resulting in asphaltene deposition are temperature, pressure and compositional changes (Ghanavati *et al*, 2013).

Effect of fuel oil to solvent ratio

The rate of deposition of asphaltene particles increases with the solvent-to-heavy fuel oil ratio. The solvent is the alkane fraction and the heavy fuel oil contains the asphaltenes and maltene fraction. The higher the dilution ratio, the larger the size of asphaltene flocs as the flocculation phase is extended (Husin *et al*, 2018). The quantity of deposited asphaltenes and deposition rate increases as the solvent-to-fuel oil ratio is increased, but decreases once the solvent-to-fuel oil ratio has surpassed the critical ratio (Husin *et al*, 2018). Figure 11 shows the effect of solvent-to-fuel oil ratio on amount of asphaltenes precipitation. A number of methods suggests the use of solvent-to-fuel oil ratio of 40:1 volume to mass ratio (v/w) with contact time between 16 to 24 hours (Ancheyta *et al*, 2009: 2).

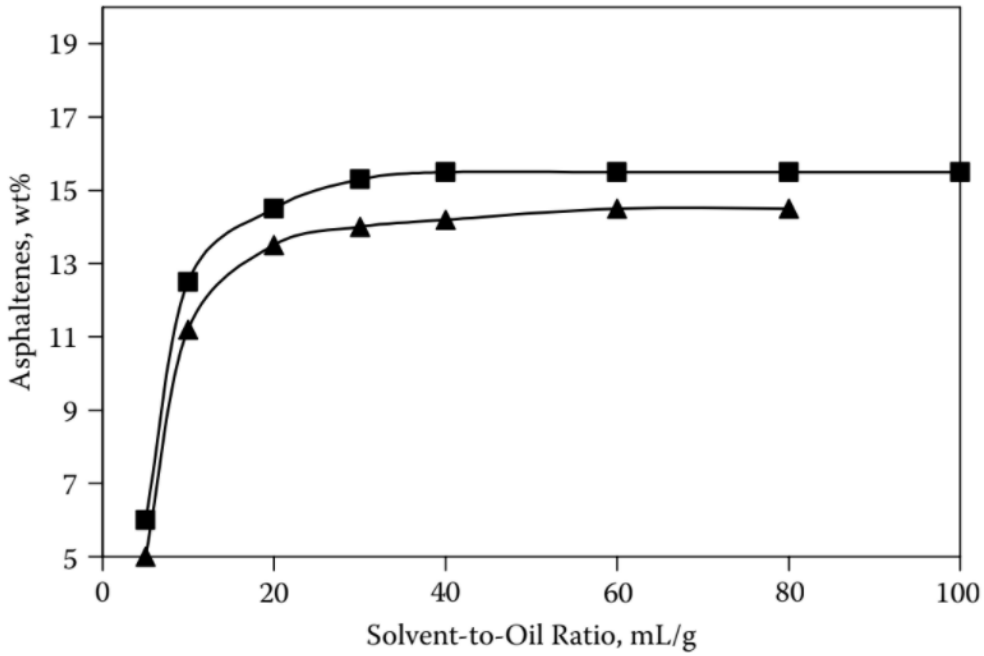

Figure 11: The amount of precipitated asphaltenes as a function of solvent-to-oil ratio ((▲) n-C_5; (■) Refinery solvent) (Ancheyta et al, 2009: 12).

Effect of temperature on solubility

Solubility of asphaltenes increases with temperature for heavy fuel oil (Mullins, 2016). As temperature increases, the asphaltene aggregate size decreases as many of the aggregates dissociate owing to higher solubility (Ualbelta, *sa*; Hemmati-Sarapardeh *et al,* 2018). Temperature has an indirect relation to asphaltene precipitation, as the surrounding temperature increases, the amount of deposited asphaltenes decreases due to fewer particle collisions as a result of higher aggregate size (Husin *et al*, 2018; Chandio *et al*, 2015). Figure 12 shows the amount of asphaltenes precipitated at different temperatures as a function of solvent-to-fuel oil ratio, which shows that at higher temperatures less asphaltenes are precipitated (Ancheyta *et al*, 2009: 12).

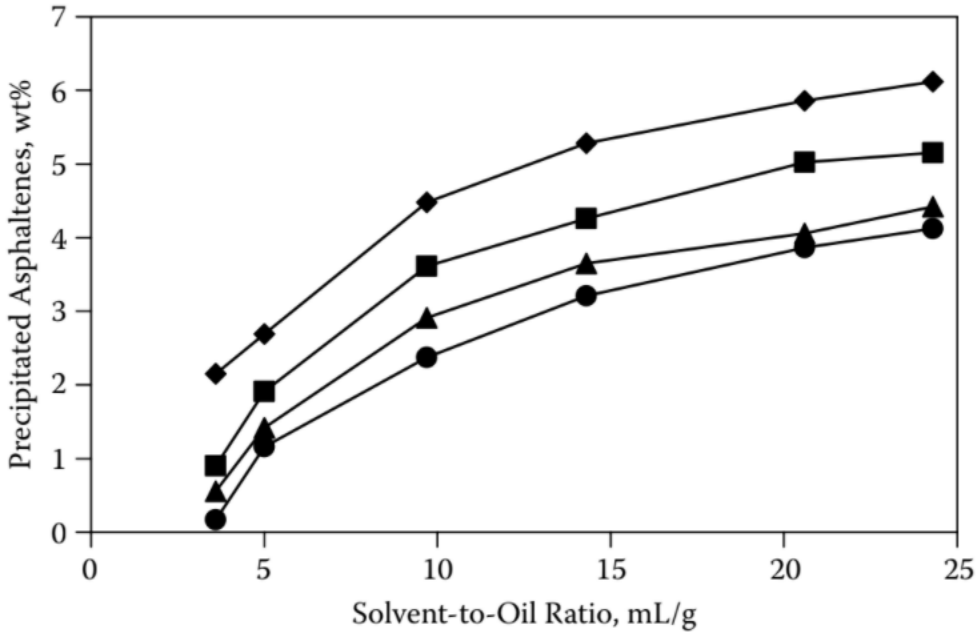

Figure 12: The amount of asphaltenes precipitated with increasing temperature using n-heptane ((◆) 25°C; (▲) 35°C; (■) 50°C; (●) 65°C) (Ancheyta et al, 2009: 13).

Precipitation of asphaltenes with waxes

Asphaltenes and waxes both have low solubility in crude oils and often precipitate together forming a composite material. Asphaltenes and waxes generate complex mixtures. The formation of the complex mixtures depend predominantly on asphaltene properties and less on the wax composition. The presence of waxes can modify asphaltene behaviour; the waxes accelerate the dissolution of asphaltenes and modify their stability (Rogel *et al*, 2016).

Asphaltenes have a great impact on wax crystallization. Asphaltene aggregates can work as nucleation sites in the crystallization process to increase the wax appearance temperature (WAT), also known as cloud point. According to Luis Alcazar-Vara, asphaltenes “promote steric interference among the paraffin molecules, which causes the formation of a weaker and less stable wax-crystals network, which is reflected in a lower amount of wax precipitated” (Alcazar-Vara & Buenrostro-Gonzalez, 2011). Figure 13 shows the wax precipitation for crude oil and its maltene fraction versus temperature graphs.

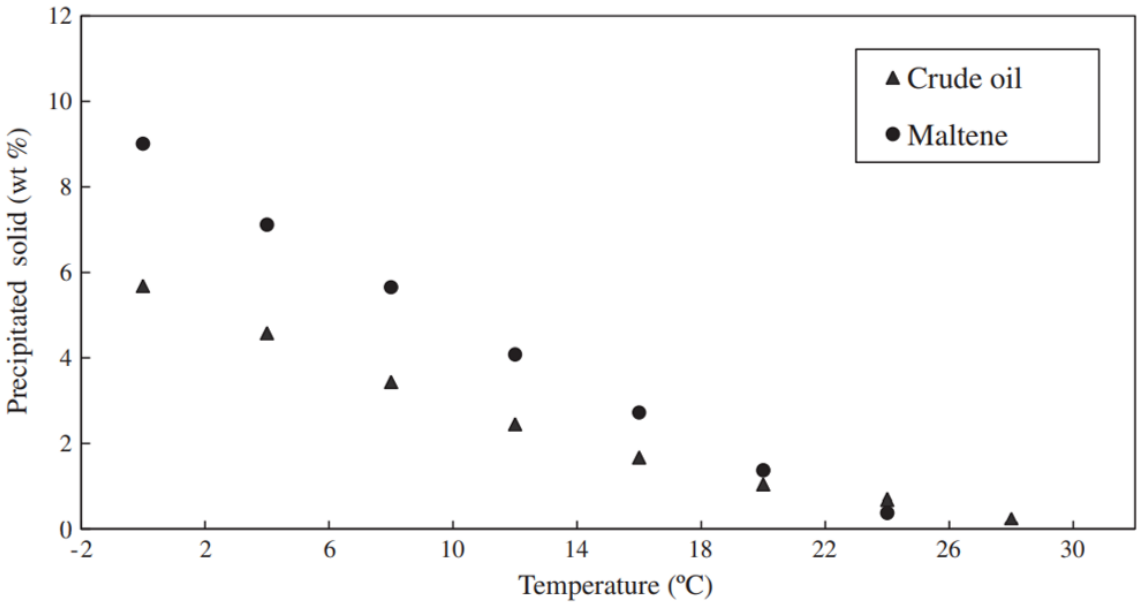

Figure 13: Wax precipitation versus temperature for crude oil and its maltene fraction (Alcazar-Vara & Buenrostro-Gonzalez, 2011).

Paraffin deposition occurs when the solid wax fraction of the paraffin oil gel increases with time in a process called aging. According to Luis Alcazar-Vara, "The gelation temperature, morphology of the gel, and its mechanical strength depend on its shear and thermal histories" (Alcazar-Vara & Buenrostro-Gonzalez, 2011). Figure 14 shows the wax to asphaltene ratio of crude oils versus the gelation and pour point temperatures. The gelation temperature and the pour point temperature both increase as wax to asphaltene ratio increases.

Table 4: Wax content and asphaltene content of crude oils (Alcazar-Vara & Buenrostro-Gonzalez, 2011).

Parameter	Crude Oil		
	A	B	C
Wax Content (wt %)	15.06	10.17	13.77
Asphaltenes content (wt %)	0.01	0.01	0.31
Wax to Asphaltene ratio	1506	1017	44.4

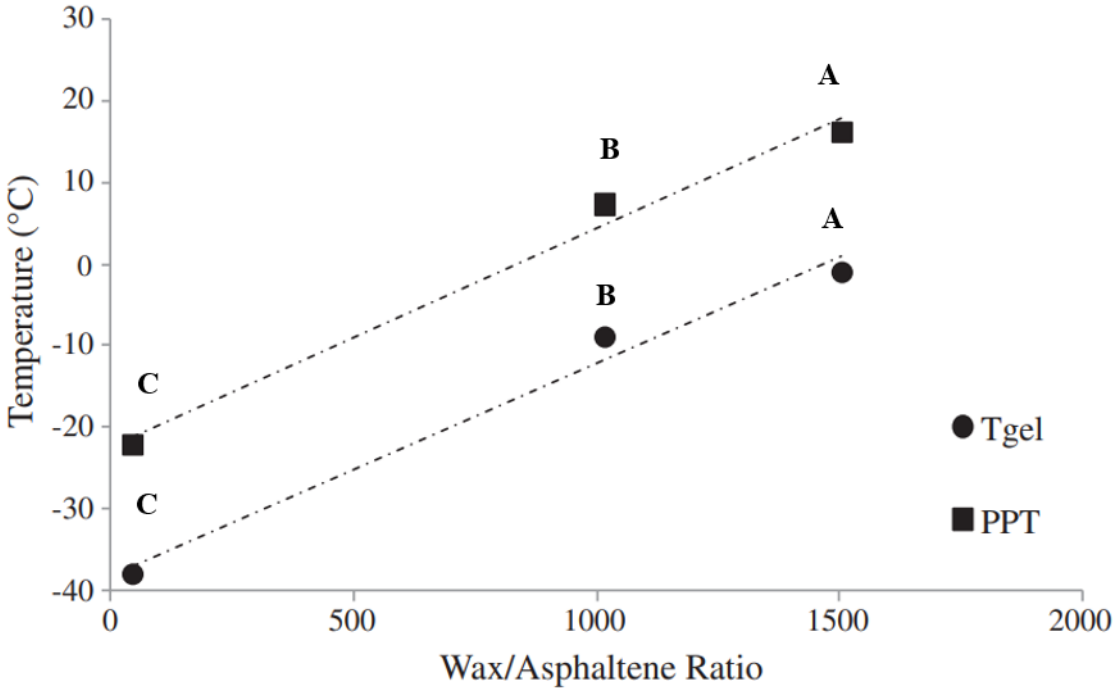

Figure 14: The effect of wax to asphaltene ratio on gelation and pour point temperatures for crude oils (Alcazar-Vara & Buenrostro-Gonzalez, 2011).

Waxes in a crude oil start to crystalize out of the solution and start to build a 3D network with a complex morphology when the surrounding temperature is lower than the WAT. Wax precipitation significantly increases the crude oil viscosity and gradually changes its flow properties at temperatures below WAT from Newtonian to non-Newtonian behaviour. Waxy crude oil behaves as a simple Newtonian fluid above the WAT. This transition from a fluid to a wax typically occurs about 10-15 °C below the WAT which may vary depending on the wax content of the crude oil (Alcazar-Vara & Buenrostro-Gonzalez, 2011).

2.5.4.4.3 Viscosity

Asphaltenes play a major role in the high viscosity behaviour of the heavy fuel oils (Ghanavati *et al*, 2013). Properties of heavy fuel oils show that, the polar fractions, more specifically asphaltenes have been identified as the cause of the rheological behaviour (Altoé *et al*, 2014). Asphaltenes reduces the economic value of crude oil. As asphaltene content increases from 0% to 40%, the crude oil's viscosity and density increase drastically and the crude oil changes colour from clear to dark brown. (Mullins, 2016). Viscosity depends directly and exponentially on asphaltene content. Experimental results where asphaltenes were removed from heavy fuel oils and then

added back to the maltenes indicate that viscosity of the reconstituted heavy oil samples increased exponentially as the asphaltenes content increased at constant temperature. The viscosity of the heavy oil samples decreases drastically with increasing temperatures at constant asphaltene volume fraction. Figure 15 shows an increase in the asphaltene content at constant temperature, the viscosity of the reconstituted heavy fuel oil increases, particularly at low temperatures (Ghanavati *et al*, 2013).

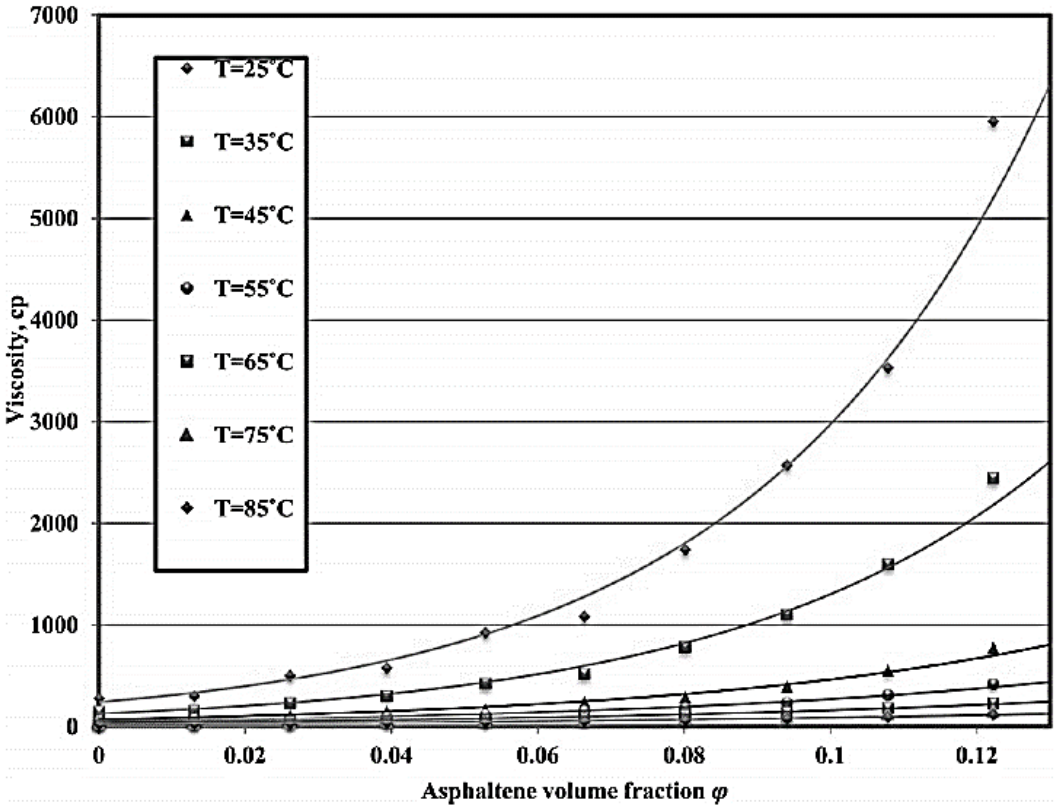

Figure 15: Viscosities of reconstituted heavy fuel oil versus asphaltene volume fraction at different temperatures (Ghanavati *et al*, 2013).

2.5.4.5 Water content in fuel oils

Water and lubricant interaction is undesirable, though it is unavoidable. The water content in fuel cannot be zero; there is always some water that is soluble in the fuel (Kirk, 2015). Water can accelerate oil oxidation resulting in corrosive and corrosion-enhanced wear (Soltanahmadi *et al*, 2017). In fuel, the solubility of water molecules depends on the humidity and the hydrophilic nature of the fuel. The water solubility increases with the environmental humidity and decreases with the sample

temperature, therefore humidity and temperature are important parameters that affect the water content and lubricity of fuel oils (Hudedagaddi *et al*, 2017).

2.5.4.5.1 Forms of water in fuel oils

There are three forms of water contamination in fuel oils namely: dissolved water, emulsified water and free water. Dissolved water in fuel oil is defined as water molecules that are dispersed throughout the fuel oil. An emulsion is defined as two immiscible liquids, where one liquid (dispersed phase) is dispersed as small droplets in another liquid (continuous phase). In the case of water in fuel oil emulsion, the water droplets are dispersed in the fuel oil (Wong *et al*, 2018). Free water in fuel oils are water molecules that are freely available. Free water remains in a distinct and separate liquid phase to the fuel oil (Mettler-Toledo, 2012).

In general free water is expected to influence lubricity more negatively than dissolved water. The free water on the metal surface results in corrosive reactions taking place on the metal surface. For non-polar lubricants, water results in negative effects on lubricity because non-polar molecular structures do not allow the lubricant to dissolve water. For polar lubricants, the influence of water on lubricity is not distinctly observed because polar molecules allow the lubricant to dissolve water due to the solubility rule which is 'like dissolves like" (Engelhardt *et al,* 2017).

2.5.4.5.2 Humidity

The fuel's ability to attract and hold water molecules from the surrounding environment depends on its composition (Lapuerta *et al*, 2016).

Relative humidity is defined by the ratio of the partial pressure of vapour in the gas mixture (P_w) to the partial pressure of vapour in the gas mixture if the gas is saturated at the given temperature of the mixture (P_s) (Himmelblau & Riggs, 2013: 624).

$$\% RH = \frac{P_w}{P_s} \times 100 \quad (4)$$

The vapour pressure of water, or saturation vapour pressure, increases strongly with temperature. For temperature range of -50-150 °C and pressures below 1000 kPa, water vapour practically behaves like an ideal gas (Rotronic, 2005).

3 Experimental

3.1 Experimental design

This section details the experimental plan for the fuel oil samples selected for this investigation. Experiments were designed to measure physical and chemical properties and then followed by friction and wear testing under various operating conditions. Triplicate test runs were performed for most experiments to ensure consistent results. The details are discussed in the following subsections.

3.1.1 Viscosity measurements

Dynamic viscosity measurements were performed for unfiltered fuel oil samples at different temperatures in order to see the effect of temperature on the dynamic viscosity of fuel oil samples. Triplicate test runs were performed. Table 5 shows the test matrix for the dynamic viscosity measurements of a fuel oil.

Table 5: Test matrix for dynamic viscosity measurements of a fuel oil sample.

Sample condition	Temperature condition	Total number of Tests
Fuel oil	15 °C	7 tests + 14 repeat tests
	25 °C	
	40 °C	
	50 °C	
	60 °C	
	80 °C	
	100 °C	

21 dynamic viscosity measurements were performed for each fuel oil sample, therefore 63 measurements in total were performed for the three selected fuel oil samples.

3.1.2 Elemental Analysis

The elemental analysis of the fuel oil samples was performed once only in order to quantify the solid particles and/or asphaltenes present in the fuel oils. Repeat runs were performed to confirm results where the actual results and the expected results had differences.

3.1.3 Water content analysis

Triplicate test runs were performed for water content measurements for fuel oil samples to confirm whether the results are reliable and consistent.

3.1.4 Precipitation of asphaltenes

Precipitation of asphaltenes from fuel oil samples was performed to remove solid particles and/or asphaltenes. The filtered fuel oil samples were used for lubricity testing. Triplicate test runs were performed in order to confirm reliability of results.

3.1.5 Lubricity tests

Lubricity tests were performed for unfiltered and filtered fuel oil samples at different temperatures and atmospheric conditions in order to see the effect of the presence of asphaltenes in fuel oils and the effect of oxidative wear. Table 6 shows the test matrix for lubricity tests of a fuel oil.

Table 6: Test matrix for the lubricity tests of a fuel oil sample.

Sample condition	Atmospheric condition	Temperature Condition	Total number of tests
Unfiltered fuel oil	Air	25 °C	12 tests + 24 repeat test
		60 °C	
		100 °C	
		115 °C	
Filtered fuel oil	Air	25 °C	
		60 °C	
		100 °C	
		115 °C	
Unfiltered fuel oil	Nitrogen	25 °C	
		60 °C	
		100 °C	
		115 °C	

36 lubricity tests were performed for each fuel oil sample, therefore 108 tests in total were performed for the three selected fuel oil samples.

3.2 Experimental Procedure

This section demonstrates details about the fuel oil samples selected for this investigation. Physical and chemical properties where confirmed and then followed by friction and wear testing under various operating conditions. The details are discussed in the following subsections.

3.2.1 Viscosity measurements

The Anton Paar SVM 3000 Stabinger viscometer was used to measure the dynamic viscosity of unfiltered fuel oils at different temperatures. A clean syringe was used to insert the fuel oil sample into the viscometer and then heated to the required temperature.

3.2.2 Elemental analysis

Elemental analysis was considered in order to characterize the elemental composition of the fuel oils. Elemental analysis of the fuel oils was performed using a Spectro Arcos inductively coupled plasma (ICP) machine from Ametek Materials Division which uses a technique known as ICP-OES (Inductively coupled plasma-optical emission spectrometry). The elemental analysis was performed on unfiltered and filtered fuel oil samples. The preparation method used for the ICP-OES was the wet-ashing procedure. A mass of 2 g of fuel oil sample was weighed in a platinum crucible. 2 ml of sulphuric acid (98%) was slowly added into the crucible and mixed with the fuel oil. The sample was incinerated at 550 °C for 2 h. Once the crucible had cooled down, the ash was dissolved in 1.5 ml of nitric acid and then diluted with 40 g of distilled water (Tekie *et al,* 2015).

3.2.3 Water content analysis

3.2.3.1 Karl Fischer

Water content analysis of fuels oils was necessary to establish if any of the selected fuel oils contain water since it was established from literature that the presence of water in fuel oils influences wear behaviour. The Karl Fischer (KF) method is one of the most frequently used titration methods for water content determination. The KF chemical reaction described in Equation 5 is used for water determinations in a non-aqueous system containing excess of sulphur dioxide (Mettler-Toledo, 2012).

$$ROH + SO_2 + R'N \rightarrow [R'NH]SO_3R + H_2O + I_2 + 2R'N \rightarrow 2[R'NH]I + [R'NH]SO_4R \quad (5)$$

The alcohol (ROH) reacts with sulphur dioxide (SO_2) and the base (R'N) to form an intermediate alkylsulfite salt ([R'NH]SO_3R), which is then oxidized by iodine (I_2) to form an alkylsulfate salt ([R'NH]SO_3R). The KF titration measures free water in the samples, the water molecules in the samples need to be freely available in order to undergo the chemical reaction with the KF reagents (Mettler-Toledo, 2012).

3.2.3.2 Method

The water content measurements were performed using the Metrohm 870 KF Titrino+. The apparatus is a titrator for water determination according to the KF-method described above. The one-component volumetric KF titration was used for the water content determination. For the one-component volumetric KF, the titrating reagent (Combititrant or composite) contains all the chemicals needed for the KF reaction, namely iodine, sulphur dioxide and the base, dissolved in a suitable alcohol. The titrating reagent is added to a solvent containing the sample by the titrator's burette during the titration. Water is quantified by the volume of KF reagent consumed. Volumetric titration is best suited for determination of water between 0.01% (100ppm)-100%. A mixture of 50% methanol and 50% chloroform was used as the solvent in the titrating cell. Chloroform is used for petroleum oils as petroleum products are hardly soluble in methanol. Chloroform can dissolve heavy petroleum oils better than the lighter solvent (e.g methanol only) and therefore exposes free water in the petroleum oil for reaction with iodine (Mettler-Toledo, 2012).

The KF apparatus dispenses the KF titrating agent containing iodine into the cell using the burette. Once all of the water present is consumed, the volume of iodine present is detected by a double platinum pin indicator electrode which signals the end-point of the titration. The equipment then calculates the end result using the on-board microprocessor. The amount of water present in the sample is calculated based on the amount of KF reagent consumed in the titration and the concentration of iodine in the KF titrating agent (titer) (Mettler-Toledo, 2012).

The titer determination was performed three times by titration of the standard (hydranal CRM water standard 10). The mean value was stored as the titer. After the titer determination, the KF determinations were performed.

The water content (WC) percentage of the fuel oils was calculated using Equation 6 (Scaccia, 2005)

$$WC = V_{KF} W_{eq} \frac{100}{W_{sample}} \quad (6)$$

where V_{KF} is the consumption of the titrant in mL, W_{eq} is the titer of the titrant in mg H_2O and W_{sample} is the weight of the sample in mg.

3.2.4 Precipitation of asphaltenes

3.2.4.1 Method

3.2.4.1.1 Precipitation procedure

Asphaltene fractions and solid particles were removed by precipitation from three fuel oils by treatment with a non-polar hydrocarbon solvent (n-heptane) (Zuo *et al*, 2019). A sample of 10 mL of fuel oil was mixed with 400 mL of 99% purity n-heptane. The mixture (fuel oil + n-heptane) was stirred for 24 h at 25 °C with a stirrer speed of 250 rpm and then allowed to settle for approximately 3 h at 25 ºC (Ancheyta *et al*, 2009: 1). It was ensured that the beaker is covered using a watch glass throughout the stirring and settling period to reduce the rate of evaporation of n-heptane. Although LFO does not contain asphaltenes because LFO is a distillate fuel oil, the solid particles in LFO were removed as the asphaltenes filtration procedure detailed below does not only remove asphaltenes but removes solid particles too.

All apparatus that was used for the asphaltenes precipitation were cleaned thoroughly before use. The apparatus was rinsed thoroughly with hexane and then dried in an oven at 90 °C for 2 minutes. Once the apparatus was cooled off, the apparatus was then rinsed with acetone and dried in the oven at 90 °C. The dried apparatus was left to cool off before use.

3.2.4.1.2 Vacuum filtration procedure

The precipitated asphaltenes (if any) as well as solid particles were separated from the remaining fuel oil and solvent mixture by vacuum filtration through two 0.2 micron

nylon membrane filters. For the vacuum filtration setup shown in Figure 16, the 0.2 micron nylon membrane filters were placed in an oven at 110 °C for 10 minutes to eliminate moisture. After the 10 minutes, the filters were weighed individually and then placed on the mesh. The mesh and the metal piece fixed together using two bolts, the bolts were properly tightened to avoid leaks during filtration. The long tube was then fixed to the mesh and metal piece using the o-ring. The filters covered the mesh and the o-ring was placed properly to avoid leaks. The long tube which is attached to the mesh and metal piece was placed on a Büchner flask and secured using a retort clamp on the retort stand. The pump is connected to the Büchner flask and switched on to start the filtration process.

Once the fuel oil and n-heptane mixture was poured into the long tube, the asphaltenes and solid particles were separated by vacuum filtration at room temperature for approximately 24 h for LFO and HFO and approximately 36h for MFO (MFO have waxy precipitants which take longer to separate from the asphaltenes). It was ensured that the vacuum filtration remained on for 24 hrs for LFO and HFO and 36 hrs for MFO even though the filtration may have been completed earlier - this aids in the separation of the maltenes and the n-heptane (evaporation of n-heptane). During filtration, minimal loss of filtration volume was observed due to the suction of the vacuum pump. Some of the waxes from MFO were left behind when transferring to storage containers. After filtration, the filter papers were dried in an oven at 110 °C (higher than boiling point of n-heptane) for 15 minutes to make sure that the asphaltenes and filter papers are completely dry. The filter papers were removed from the oven to cool off and then weighed. The filtered mixture was poured into a container and left in the desiccator for 24 hours, ensuring that the mixture container was open to allow the evaporation of the remaining n-heptane. After 24 hrs, the container was closed for storage until required for the HFRR friction and wear testing.

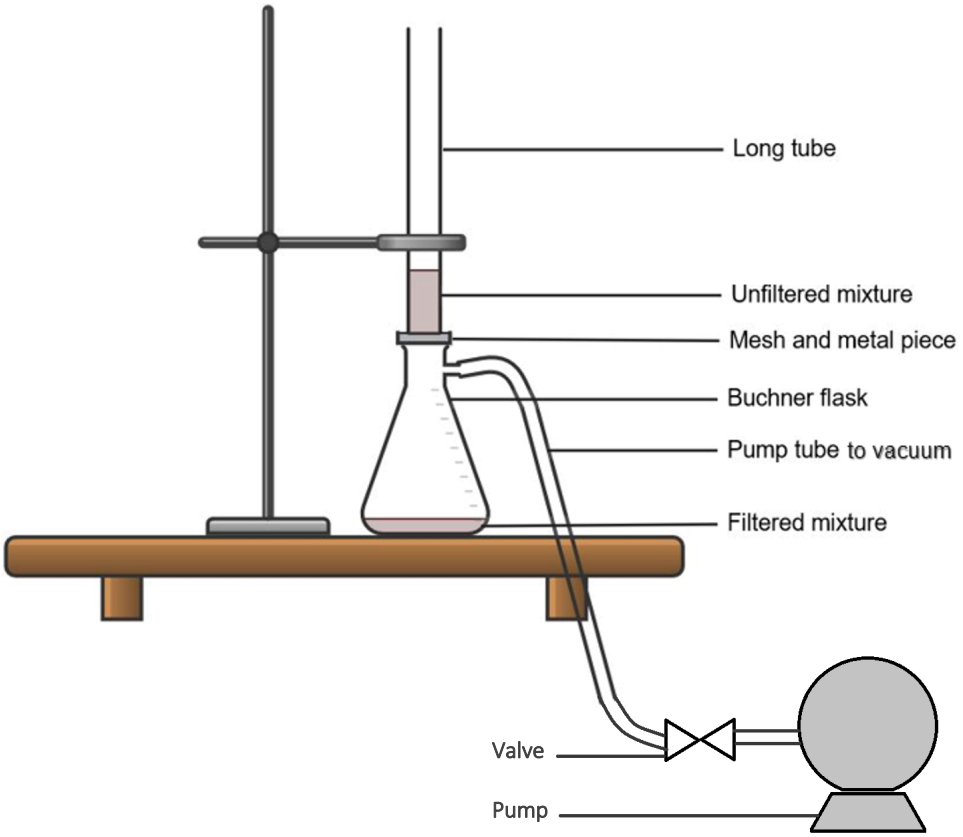

Figure 16: Diagram of the asphaltene vacuum filtration setup.

During the testing of the vacuum filtration procedure, the filters used were 0.8 micron nylon membrane filters. This filter size was too big since from visual inspection of “filtered fuel oil” showed that particles were still present. This is an indication that most of the asphaltenes particles are below 0.8 micron and therefore a smaller filter size was required. The 0.8 micron nylon membrane filters were replaced with 0.2 micron nylon membrane filters. During the testing of the vacuum filtration procedure, after filtration of the fuel oil, the Büchner flask was heated to 50 °C in order to decrease the viscosity and therefore remove most of the filtered fuel oil for storage for use in friction and wear testing. Heating of the filtered fuel oils resulted in increased viscosity for filtered MFO, which contains waxes, when the sample cooled down. The filtrates were removed from the Büchner flask without heating so the physical properties would remain the same.

3.2.5 Lubricity tests

3.2.5.1 Tribometer: HFRR

In this study, lubricity was determined using the high frequency reciprocating rig (HFRR) test due to its ability to provide a broad range of wear mechanisms related to adhesion (Lapuerta *et al*, 2016). The HFRR is a reciprocating friction and wear test machinery which assesses repeatable performance of fuels and lubricants. The HFRR is suitable for the wear testing of relatively poor lubricants and for boundary friction measurements and has become the industry standard test for diesel fuel lubricity because diesel fuel is a relatively poor lubricant (Mang & Dresel, 2017: 914; PCS Instruments, *sa*). The HFRR produces results via measurements of the continuous friction force, the contact resistance (film) and the test fluid temperature values. The components of the machinery compose of a mechanical unit, control unit and a computer. The control unit is connected to a computer for data logging, graphical representation of test parameters and results storage (PCS Instruments, 2005). Figure 17 shows the schematic of the HFRR machine.

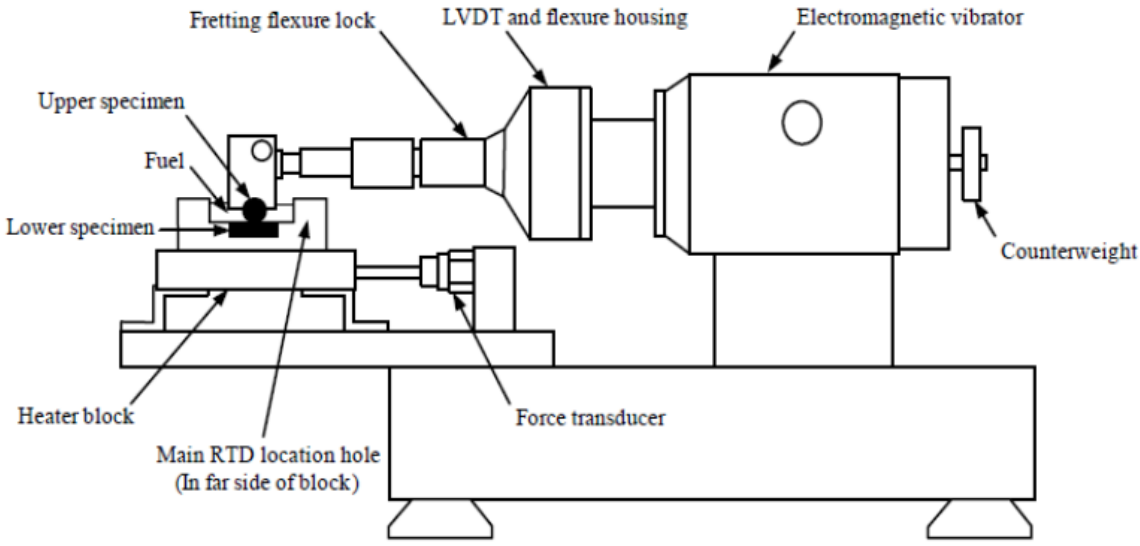

Figure 17: Schematic of the HFRR machine (Doustdar *et al*, 2016).

The HFRR tribometer has a ball on disk contact configuration shown in Figure 18. The detailed configuration and operating conditions are given in Table 7 below.

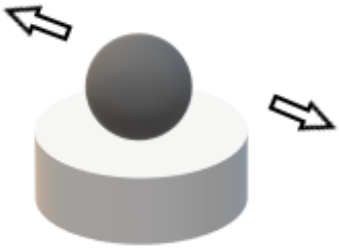

Figure 18: The ball on disk contact configuration for the HFRR machine.

Running-in and steady state wear are the different stages that occur during the lifetime of components. The largest amount of material loss takes place during running-in. In the running-in stage, plastic deformation on the surface asperities and removal of material occurs resulting in surface roughness changes. Severely-loaded systems during the running-in stage result in severe wear without reaching a steady state stage where mild wear conditions occurs (Bosman *et al*, 2011).

3.2.5.1.1 Electrically insulating film

Electrical contact resistance (ECR) can be utilized as a qualitative indicator for film formation. The extent of direct metal-to-metal contact can be indicated by the ECR values between two contacting surfaces although deducing the real area of contact by the ECR is not clear (Viesca, 2010).

The electric conductivity of a fuel oil is a measure of a fluid's electrostatic chargeability. Conductivity is dependent on the type of fluid as well as the concentration of movable charge carriers. The more polar a fuel oil is, the more conductive the fuel oil. The fuel oil's conductivity increases with increasing proportion of metal-organic additives. The lubricants' conductivity is also influenced by temperature, the increase in temperature results in increasing fuel oil's conductivity. This relationship is not linear. Each fuel oil has its own conductivity vs temperature relationship. At constant temperature, conductivity varies throughout the friction and wear test as a result of wear materials, impurities such as water, chemical reactions, and oxidation and aging products (Lindner, 2013).

A low or zero film reading of the film means that the contact resistance is very low due to major solid-solid contact taking place on the contacting surfaces (the ball and disk). This is generally related to high coefficient of friction and wear. A high film reading

indicates the separation of the metal surfaces by the lubricant. This may be due to chemical film formation or by formation of a partial hydrodynamic film if specimen speed and fluid viscosity are high enough (PCS Instruments, 2005).

3.2.5.1.2 Operating conditions

The operating conditions of the HFRR tests are given in Table 7. The test specimens for the HFRR tests, ball and disc, conform to all international diesel fuel test standards (PCS Instruments, 2005).

Table 7: The operating conditions of HFRR (PCS Instruments, 2005*;* PCS Instruments, 2020).

Operating conditions	Value
Frequency	10 - 200 hz
Stroke length	20 µm - 2 mm
Load	0.1 to 1 kg
Maximum friction force	10N
Upper specimen	6 mm diameter ball
Lower specimen	10 mm diameter x 3 mm thick disc
Material of ball	ANSI E-52100
Material of disc	AISI E-52100
Surface roughness of ball	< 0,05 µm R_a
Surface roughness of disc	< 0,02 µm R_a

3.2.5.1.3 Corrected wear scar diameter

The relative humidity in the HFFR chamber influences the lubricating properties of the fuel and therefore the wear scar size in the HFRR test, especially when oxidative wear is predominant. According to the ISO 12156-1 standard, a humidity correction factor (HCF) of 60 µm(kPa)$^{-1}$ is proposed for all the fuels as a correction of the vapour pressure, regardless of their composition (Lapuerta *et al*, 2016). The uncorrected wear scar diameter is given by Equation 7 according to ISO 12156-1

$$MWSD = \frac{(x + y)}{2} \quad (7)$$

where x is the wear scar measurements perpendicular to the oscillation direction and y is the wear scar measurements parallel to the oscillation direction. The corrected wear scar diameter ($WS_{1.4}$) calculation is expressed by the following equations (ISO 12156-1, 2006). The initial absolute vapour pressure and the final absolute vapour pressure, AVP_1 and AVP_2 respectively, in kPa, are calculated using the Equation 8

$$AVP_i = \frac{RH_i \times 10^{v_i}}{750}, i = 1,2 \quad (8)$$

where RH_1 is the relative humidity at the start of the test and RH_2 is the relative humidity at the end of the test, in percentage. The calculation for v_1 and v_2 is expressed in Equation 9

$$v_i = 8.017352 - \left(\frac{1705.984}{231.864 + T_i}\right), i = 1,2 \quad (9)$$

where T_1 and T_2 are the air temperatures at the start and end of the test respectively. The mean absolute vapour pressure during the test is calculated using Equation 10.

$$AVP = \frac{AVP_1 + AVP_2}{2} \quad (10)$$

The equation used to calculate the corrected wear scar diameter is Equation 11

$$WS_{1.4} = MSWD + HCF(1,4 - AVP) \quad (11)$$

where HCF=60 for unknown fuel samples. The $WS_{1.4}$ is still required for lubricity test results although the latest ISO 12156-1 standard does not require the $WS_{1.4}$ anymore. The latest SANS 342 specification for diesel still requires the $WS_{1.4}$ for lubricity test results (ISO 12156-1, 2018; SANS 342, 2016).

3.2.5.2 Test conditions

Friction and wear tests were performed according to ISO 12156-1 on the HFRR under atmospheric air for filtered and unfiltered fuel oil samples and under inert nitrogen atmosphere for unfiltered fuel oil samples. In order to report on the effect of temperature, the HFRR tests were performed at different temperatures (25, 60, 100 and 115 °C). The summary of the test conditions are shown in Table 8.

Table 8: HFRR test conditions

Parameter	Value
Stroke length, mm	1 ± 0.02
Frequency, Hz	50 ± 1
Humidity, % (RH)	50 ± 5 (Air), 15 ± 5 (N_2)
Fluid temperature, ºC	115 ± 2, 100 ± 2, 60 ± 2, 25 ± 2
Load, g	200 ± 1
Test duration, min	75 ± 0.1
Fluid volume, ml	2 ± 0.2
Reservoir surface area, mm^2	600 ± 100

The specimens were cleaned using toluene and acetone before the HFRR test. The detailed cleaning procedure is in Appendix A1. The HFRR tribometer was cleaned using hexane and then acetone before the assembly of the HFRR configuration shown in Figure 19.

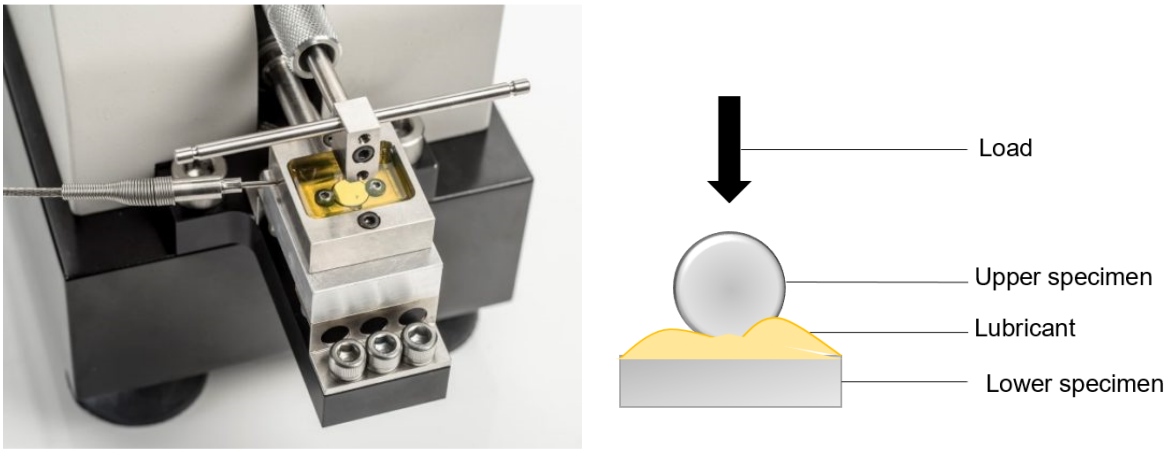

Figure 19: HFRR configuration (PCS Instruments, 2020).

The lubricity tests for the different fuel oil samples were performed at 25, 60, 100 and 115 °C. The lubricity tests were performed at 25 °C because it is the standard test temperature for lubricants where there may be concerns about loss of oil because of its volatility or degradation. Gasoline lubricity tests are performed at 25 °C due to their high volatility (ASTM D6079, 2011). The lubricity tests were also performed at 60 °C because it is the standard test temperature for diesel fuels according to the ISO 12156-1 standard (ISO 12156-1, 2006). The test temperature of 100 °C was selected for the

lubricity tests because residual fuel oils for industrial use get preheated to 77-104 °C before being pumped into the burner for proper atomization at the burners, 100 °C was selected because it is the rounded upper range (Al Fanar Petroleum Oil Trading). It was also decided to include a higher temperature than the temperature at which the fuel oil is preheated before being pumped into the burner in order to see how the fuel oils would perform at the higher temperature. The 115°C HFRR runs were performed simply to confirm that the investigation should not go beyond the normal boiling point of water. Expected evaporation takes place at 115°C because the fuel oils contain certain amounts of volatiles. The results at 115°C do not contribute to understanding of the temperature effects on fuel oils, which is seen by the change in trend at 115°C in the HFRR results below.

The lubricity tests were chosen to be performed on filtered and unfiltered fuel oils. The fuel oils were filtered to investigate how the fuel oils would be perform without the presence of solid particles and/or asphaltenes. This helps to distinguish the impact of the solid particles and/or asphaltenes on the lubricity of fuel oils. The comparison of the filtered and unfiltered fuel oils lubricity results will give an indication of the role of the solid particles and/or asphaltenes on the lubricity of the different fuel oils.

Two atmospheres were chosen: the oxidizing (air) atmosphere and the inert (nitrogen) atmosphere. The change in environment will allows us to distinguish the impact of oxidation on the fuel oils. Oxidation products form an oxide film on the contacting metal surfaces which tends to slow down or even arrest oxidation. This will be done by comparing the unfiltered fuel oils lubricity test under the oxidizing (air) atmosphere to the inert (nitrogen) atmosphere. The 50% RH under air atmosphere was selected because the humidity is within the acceptable laboratory air conditions for a standard lubricity test according to the ISO 12156-1 (ISO 12156-1, 2018). The 15% RH under nitrogen atmosphere was selected because this was the lowest consistent humidity that could be achieved throughout the test since the chamber is not a completely closed system as gaseous emissions leave the chamber throughout the test.

A humidifier was used to control the relative humidity of the HFRR chamber to 50% RH under atmospheric air and 15% RH under inert nitrogen. The humidity was monitored throughout the HFRR test using a Sensirion SHT2x humidity sensor since

the chamber is not a completely closed system as some gaseous emissions leave the chamber throughout the test.

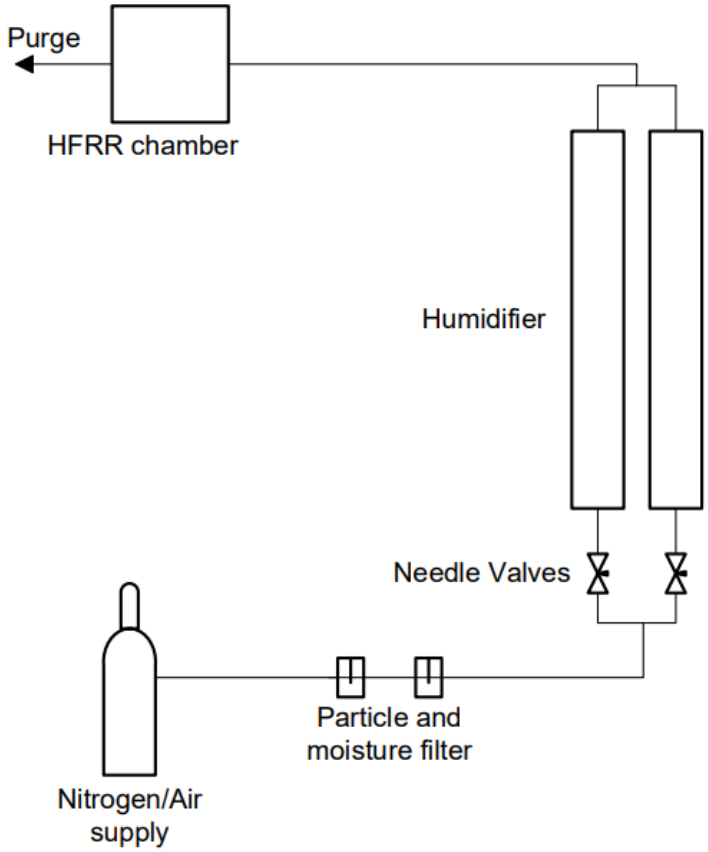

Figure 20: Humidifier assembly

Air/nitrogen supply passes through moisture and particle filters. For 50% RH under atmospheric air, the wet air from the bubbler and dry air from the dryer mix to give the required relative humidity in the HFRR chamber. For 15% RH under inert nitrogen, the bubbler was switched off and dry nitrogen from the dryer was used to achieve the required relative humidity in the HFRR chamber. The flow rates of the bubbler and dryer were controlled by adjusting the needle valves throughout the test as shown in Figure 20.

3.2.5.3 Wear scar measurements

A Zeiss Axio Scope.A1 polarized light microscope with a digital AxioCam ERc 5s camera was used to obtain micrographs of the wear scars. The wear scars were measured using an AxioVision 4 software. The pictures of the ball scar and disk track were taken and the wear scar diameters were measured in the x-direction,

perpendicular to the oscillation direction and the y-direction, parallel to the oscillation direction. The ball scar and disk track were always measured with the same orientation. For the ball scar measurements, the screw of the upper specimen holder was always facing away from the microscope. For the disk track measurements, the lower specimen temperature probe hole was always placed on the left hand side and away from the microscope.

For the ball scar measurement, the microscope table was levelled by adjusting the knob before use and then the 10x magnification lens was selected. The Axiovision software was then opened and the magnification was set to 10x on the software. The ball was placed so the horizontal wear scar diameter of the ball was perpendicular to the sliding direction and the vertical wear scar diameter of the ball was parallel to the sliding direction before taking measurements.

For the disk track measurement, the microscope table was levelled by adjusting the knob before use and the 5x magnification lens was selected. The Axiovision software was then opened and the magnification was set to 5x on the software. The disk track was placed horizontally on the microscope table before taking measurements.

4 Results and discussion

4.1 Viscometer measurements

The dynamic viscosity of the unfiltered fuel oils at different temperatures are shown in Figure 21. The results show that the viscosities of the fuel oils tested decrease exponentially with increasing temperature. The absence of asphaltenes in LFO results in lower viscosity measurements and a gentle gradient for viscosity versus temperature graph as compared to MFO and HFO.

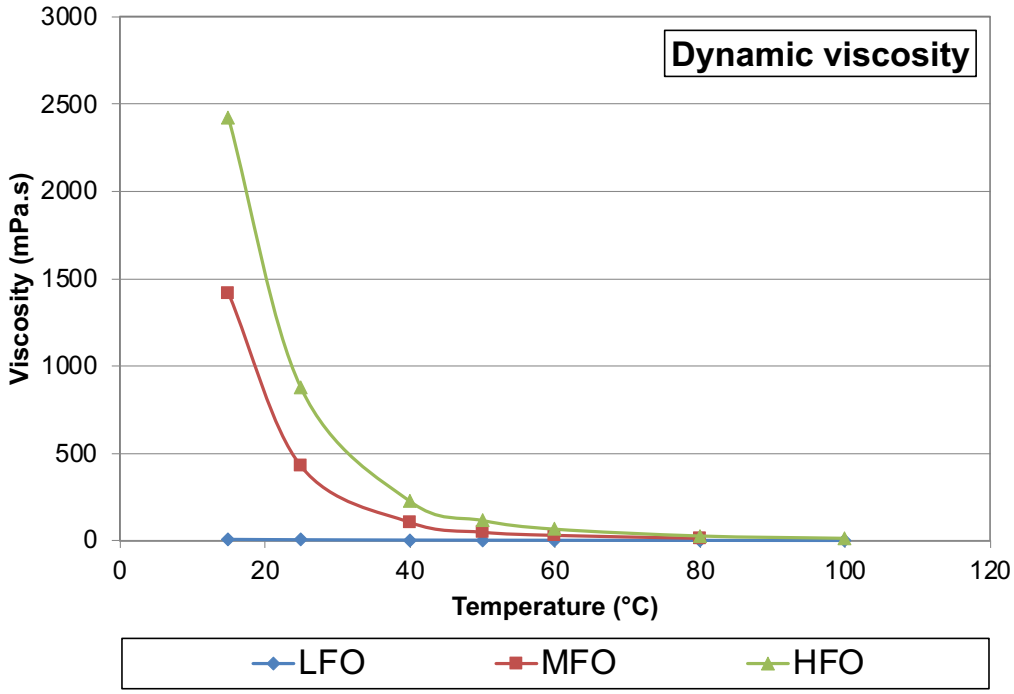

Figure 21: Dynamic viscosity of unfiltered fuel oils at different temperatures.

4.2 Elemental analysis

Table 9: ICP OES results for unfiltered fuel oils.

Sample	HFO (mg/kg)	MFO (mg/kg)	LFO (mg/kg)
V	14,7	4,94	2,15
Ni	10,5	2,37	1,61
Na	80,8	1,78	6,80
Fe	28,6	6,71	18,1
Mn	1,69	1,18	1,07
Mg	9,21	2,96	4,65
K	11,1	2,76	4,11
S	883	118	159
Cr	4,32	1,58	3,76
Ca	124	60,6	85,2
Al	216	2,37	1,79
P	18,6	-	-
Zn	9,77	2,57	3,04
Si	5,26	8,69	11,3

From the ICP-OES analyses shown in Table 9, HFO has the highest concentration of asphaltenes and solid particles compared to MFO and LFO. The asphaltene concentration is shown by the high concentration of vanadium, nickel and iron (metals found in asphaltenes) in HFO compared to MFO since LFO does not contain asphaltenes as it is a distillate fuel oil. The high metal content in LFO may be because the catalytic reactor feed was not pre-treated resulting in a low-quality light cycle oil with high concentration of metal but not asphaltenes. The silica concentration in LFO is higher compared to MFO and HFO because light cycle oils pass through a catalytic reactor which use silica as a catalyst. The silica fines remain in the LFO. MFO and HFO are fuel oils which are a mixture of oil from the catalytic reactor and oil from the bottoms of the distillation column which does not contain silica fines shown in Figure 6 and Figure 7. This results in lower silica concentration for MFO and HFO compared to LFO.

Table 10: ICP OES results for filtered fuel oils.

Sample	HFO(mg/kg)	MFO(mg/kg)	LFO (mg/kg)
V	2,82	1,26	0,219
Ni	1,60	0,709	0,310
Na	8,96	8,37	8,40
Fe	6,67	4,77	3,50
Mn	0,415	0,236	0,346
Mg	2,19	2,01	2,22
K	0,415	0,296	0,492
S	1,52	1,28	1,86
Cr	1,09	0,394	0,510
Ca	41,4	30,64	44,46
Al	1,42	0,768	0,601
P	0,138	0,887	0,237
Zn	1,05	0,788	1,04
Si	4,70	2,52	2,04

From the ICP analyses shown in Table 10, the concentration of asphaltenes and solid parts have drastically decreased for LFO, MFO and HFO compared to the unfiltered ICP OES results shown in Table 9. The abrasive particles in the fuel oils have been removed from the fuel oils, only fine particles remain in the fuel oil (<0.2 micron). The remaining asphaltenes in MFO and HFO, if any, are dispersed asphaltenes (<2 μm) (Lei *et al*, 2016).

4.3 Water content measurements

The water content results for LFO, MFO and HFO were 0.1%, 0.12% and 0.13% respectively. Results show that the water content increases with supposed increasing asphaltene content. MFO and HFO are polar fuel oils containing asphaltenes. Water content contributes to the formation of protective layer (iron oxide) and therefore improves lubrication. Although MFO and HFO have more free water, the polar species in MFO and HFO are preferentially adsorbed which prevents the formation of an oxide

layer. For LFO, the low concentration of polar compounds and reactive species tend to form an oxide layer on the metallic surfaces (Lapuerta *et al,* 2014).

4.4 Asphaltene content and solid particles measurements

The concentration of asphaltenes and solid particles from filter cake measured increases in the order LFO, MFO and HFO respectively. The concentration of asphaltenes and solid particles for LFO, MFO and HFO were 5.67 ± 1.71, 23.5 ± 0,125 and 48.7 ± 2,84 $g(L)^{-1}$ respectively. Figure 22 shows the filter cakes for the fuel oils. Note that the circular papers used to lay the precipitated asphaltenes and solids particles are the same size.

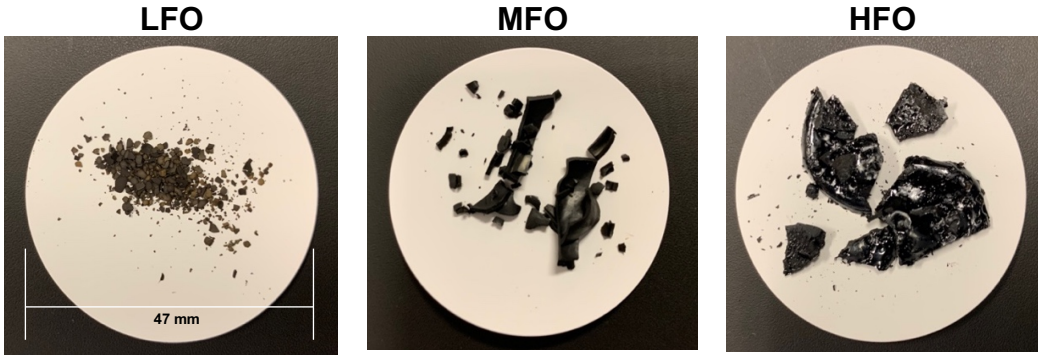

Figure 22: Precipitated asphaltenes and solid particles for the fuel oils.

4.5 Friction and wear tests

4.5.1 LFO

4.5.1.1 Coefficient of friction (LFO)

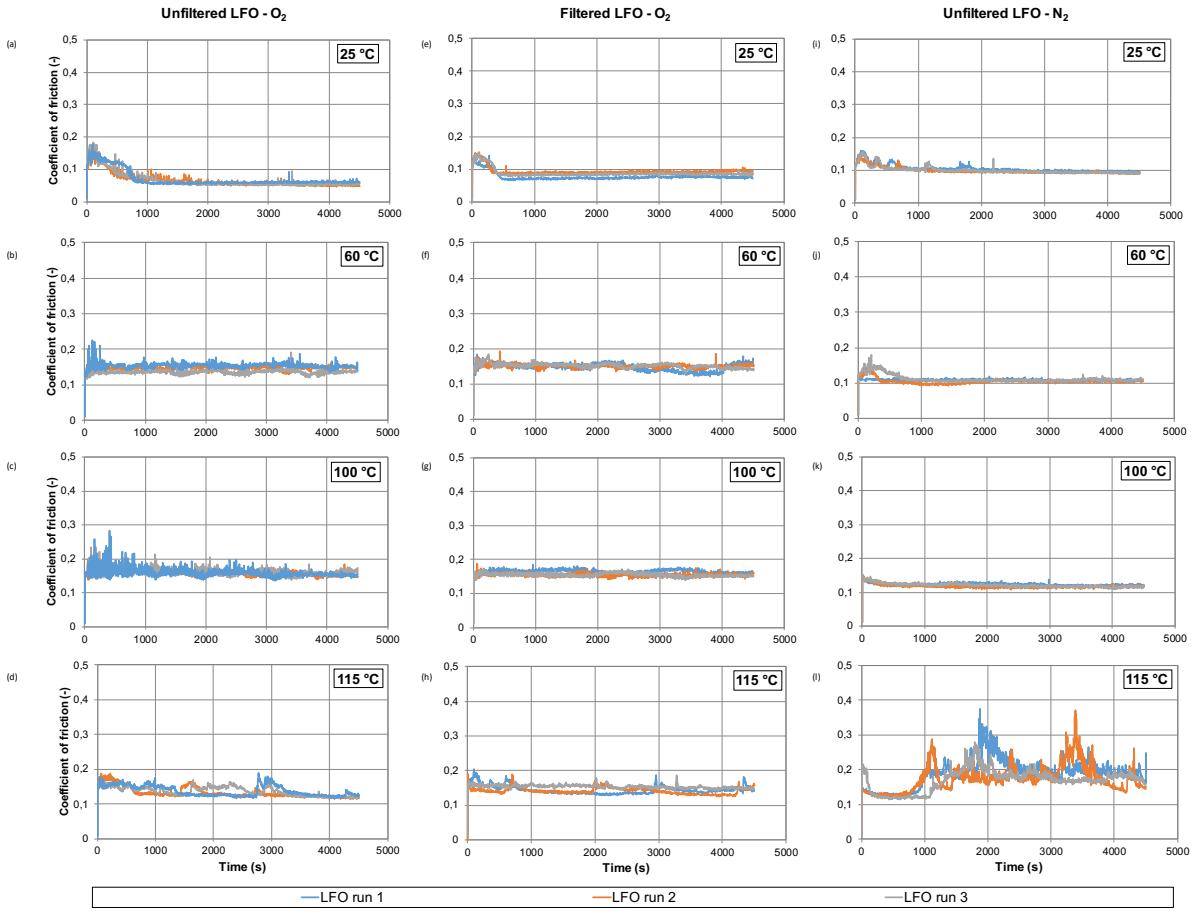

Figure 23: Coefficient of friction versus time graphs of LFO for three runs at different temperatures.

The effect of temperature (LFO)

The COF of unfiltered and filtered LFO under oxygen-rich atmosphere increases with the increase in temperature, although there is a decrease between 100 and 115 °C as shown in Figure 23(a)-(h). Unfiltered and filtered LFO under oxygen-rich atmosphere at 25 °C have the lowest COF throughout the test. This is a result of a viscosity-temperature relationship. At low temperatures the viscosity is higher resulting in a thicker film. The thicker film allows for separation between the contacting surfaces (Stachowiak & Batchelor, 2014: 11). For unfiltered LFO under oxygen-rich atmosphere, the roughness of the COF measurement increases with the increase in

temperature, although there is a decrease between 100 and 115 °C. The roughness of the COF for filtered LFO under oxygen-rich atmosphere stays relatively smooth with increasing temperature. The solid particles in unfiltered LFO under oxygen-rich atmosphere interact with the surface resulting in the concentration of heat which increases the instability of COF when compared with filtered LFO under oxygen-rich atmosphere (Stachowiak & Batchelor, 2014: 11). The presence of oxidation is also responsible for the COF instability of the filtered and unfiltered LFO under oxygen-rich atmosphere because the COF for unfiltered LFO under nitrogen atmosphere shows smooth COF results between 25 and 100 °C.

The COF for unfiltered LFO under nitrogen inert atmosphere stays relatively constant and smooth between 25 and 100 °C, although there is a drastic increase between 100 and 115 °C shown in Figure 23(i)-(h). The increase in temperature shows minimal effect on the COF of unfiltered LFO under nitrogen atmosphere, although at 115 °C, the COF values fluctuate throughout the test with high COF peaks. The high and rough COF could be due to breakthrough of the fuel oil; this will be confirmed by the wear results. Breakthrough of the fuel oil is determined by high COF and complete metal-to-metal contact.

The effect due to solid particles (LFO)

At 25 °C, the COF is drastically higher for filtered LFO under oxygen-rich atmosphere when compared with unfiltered LFO under oxygen-rich atmosphere. The removal of solid particles in filtered LFO under oxygen-rich atmosphere also removes molecules with good lubricity resulting in increased COF when compared with unfiltered LFO under oxygen-rich atmosphere (Lapuerta *et al,* 2014). Between 60 °C and 115 °C, the COF is similar for filtered and unfiltered LFO under oxygen-rich atmosphere, although the roughness of the COF for unfiltered LFO is much more severe when compared with filtered LFO especially at high temperatures. This is due to the solid particles in unfiltered LFO which interact with the surface resulting in concentration of heat at the contacts resulting in a rougher COF profile (Stachowiak & Batchelor, 2014: 11).

The effect of atmosphere (LFO)

At 25 °C and 115 °C, the COF for unfiltered LFO under oxygen-rich atmosphere is lower and has increased stability compared to unfiltered LFO under nitrogen atmosphere. At 25 °C, the slight increase in the COF for unfiltered LFO under nitrogen atmosphere when compared with unfiltered LFO under oxygen-rich atmosphere is likely due to reduced viscosity. At 115 °C, the COF decreases for unfiltered LFO under oxygen-rich atmosphere when compared with unfiltered LFO under nitrogen atmosphere where high and rough COF values occur. The lower COF for unfiltered LFO under oxygen atmosphere is due to formation of a protective layer (ferrous oxide) which protects the contacting surface resulting in reduced COF. Oxidation is predominant in LFO under oxygen atmosphere, the very low oxygen concentration and humidity in the nitrogen inert atmosphere results in high and rough COF at 115 °C for unfiltered LFO under nitrogen atmosphere due to less protection of the metal surfaces (Lapuerta *et al,* 2014: Bhushan, 2013: 359). At 60 and 100 °C, the increased roughness of the COF for unfiltered LFO under oxygen-rich atmosphere is due to the dynamic nature of the oxide formation in the presence of solid particles. This can be seen by reduced roughness of COF for filtered LFO under oxygen-rich atmosphere and no roughness of the COF for unfiltered LFO under nitrogen-rich atmosphere.

4.5.1.2 % Film thickness (LFO)

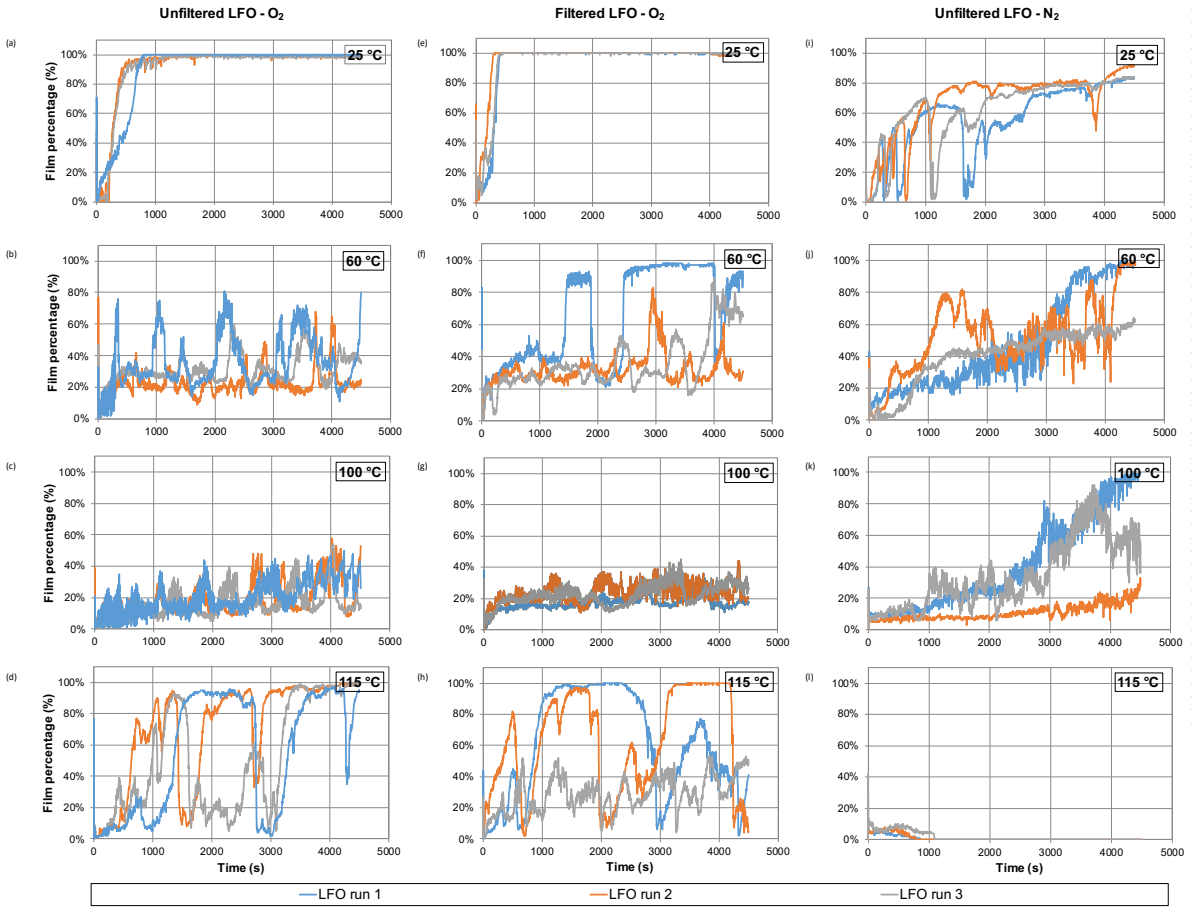

Figure 24: Film versus time graphs of LFO for three runs at different temperatures.

The effect of temperature (LFO)

For unfiltered LFO and filtered LFO under oxygen-rich atmosphere, the increase in temperature results in a decrease in % film and smoothness of % film, although there is an increase between 100 and 115 °C shown in Figure 24(a)-(h). As the temperature increases between 25 and 100 °C for unfiltered LFO and filtered LFO under oxygen-rich atmosphere, the chemical reactivity increases resulting in increased film formation rate, while the film removal rate increases due to decreased durability of the film. Unfiltered LFO and filtered LFO under oxygen-rich atmosphere show stable film results at 25 °C, this is shown by the smooth and repeatable % film results. At moderate to high temperatures (60 to 115 °C), unfiltered LFO and filtered LFO under oxygen-rich atmosphere show unstable % film behaviour.

For unfiltered LFO under nitrogen atmosphere, the increase in temperature results in the decrease in % film shown in Figure 24(i)-(l), where the % film at 115 °C is zero. Lubricants' electrical conductivity is influenced by temperature. The higher the temperature, the higher the oils' conductivity which results in the decrease in % film (Lindner, 2013). The % film at 25 °C is smooth while at 60 and 100 °C, the % film is rough in comparison with 25 °C. For unfiltered LFO under nitrogen atmosphere, the gradual increase % film with time is due to increasing film formation with time. The low concentration of water and oxygen due to the low humidity and inert atmosphere results in low film formation rate. The zero film at 115 °C could be due to breakthrough of the fuel oil; this will be confirmed by the wear results. Significant contact of surfaces and wear is expected at 115 °C.

The effect due to solid particles (LFO)

LFO containing solid particles only results in minimal change in % film for filtered LFO and unfiltered LFO at different temperatures.

The effect of atmosphere (LFO)

At 25 °C, the % film for unfiltered LFO under nitrogen atmosphere continuously breaks down and reforms when compared with the % film for unfiltered LFO under the oxygen-rich atmosphere which increases to 100%. At 60 and 100 °C, the % film for unfiltered LFO under oxygen-rich and nitrogen atmosphere shows an unstable film (film fluctuates) with the % film for unfiltered LFO under nitrogen atmosphere increasing with time while unfiltered LFO under oxygen-rich atmosphere remains around the same range throughout the test. At 60 and 100 °C, the increased roughness of the % film for unfiltered LFO under oxygen-rich atmosphere is due to the dynamic nature of the oxide formation in the presence of solid particles. This can be seen by reduced roughness of % film for filtered LFO under oxygen-rich atmosphere and no roughness of the % film for unfiltered LFO under nitrogen-rich atmosphere. At 115 °C, the % film for unfiltered LFO under oxygen-rich atmosphere breaks and reforms throughout the test while the % film for unfiltered LFO under nitrogen atmosphere is zero (Lapuerta *et al*, 2014).

4.5.1.3 Wear scar micrographs

The wear scar micrographs produced from the friction and wear tests are shown below with their respective complementary ratings (CR) and average corrected wear scar diameters ($WS_{1.4}$). The CR helps to identify different wear mechanisms which lead to different visual appearances on the ball. The CR is based on a 6-graded visual rating scale method with 1 being excellent (full) lubrication and 6 being no lubrication with distinct wear marks inside the contact (Oláh *et al*, 2005). Note that the wear scar micrographs are not to scale.

Table 11: Wear scars for LFO runs at different temperatures.

	25 °C	60 °C	100 °C	115 °C
Unfiltered LFO (O_2)	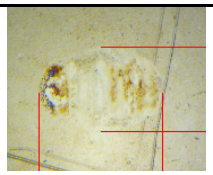	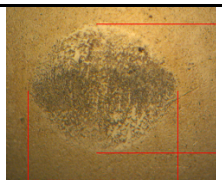	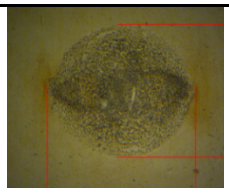	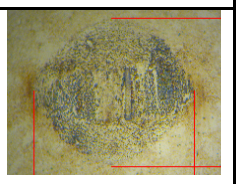
CR	3	2	3	4
$WS_{1.4}$ (µm)	191	360	364	295
Filtered LFO (O_2)	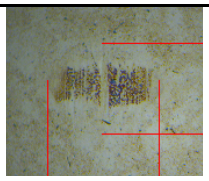	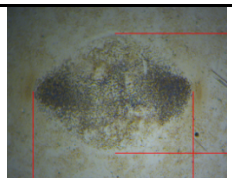	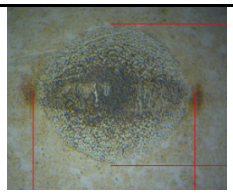	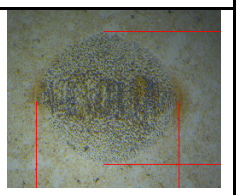
CR	3	2	2	2
$WS_{1.4}$ (µm)	145	348	375	307
Unfiltered LFO (N_2)	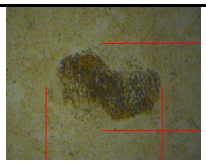	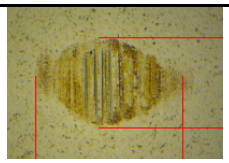	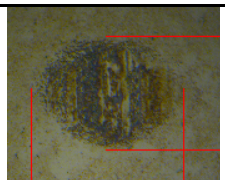	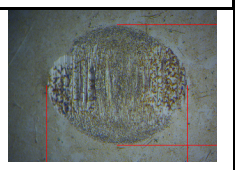
CR	2	3	3	4
$WS_{1.4}$ (µm)	238	233	245	422

The effect of temperature (LFO)

For unfiltered LFO under oxygen-rich atmosphere, the CR decreases from 25 to 60 °C and increases from 60 to 115 °C. At high temperatures slight abrasion occurs due to decrease in the viscosity which results in reduction of the film thickness and therefore less separation between the solid particles for unfiltered LFO under oxygen-rich atmosphere and metal surfaces (Stachowiak & Batchelor, 2014: 11). As the temperature increases for unfiltered LFO under oxygen-rich atmosphere, the degree of oxidation increases. This is seen by the darkening of the wear scar due to increased oxidation which causes oxide formation on the contact surface (Oláh *et al*, 2005).

For filtered LFO, the CR is the highest at 25 °C and stays constant between 60 and 115 °C at a CR of 2. Oxidative wear is the lowest at 25 °C for filtered and unfiltered LFO under oxygen-rich atmosphere because of the low temperature. Oxidative wear occurs at high temperatures (Bhushan, 2013: 359). There is no abrasion for filtered LFO under oxygen-rich atmosphere. The wear scars for filtered LFO and unfiltered LFO under oxygen-rich atmosphere look similar with filtered LFO having less abrasive wear due to the removal of solid particles. The solid particles interact with the surfaces which results in increase in CR and more wear.

For unfiltered LFO under nitrogen atmosphere, the CR increases between 25 and 60 °C and stabilizes until 100 °C and then increases. As temperature increases, abrasive wear increases. This is due to the decrease in viscosity with increasing temperature which results in the reduction of the film thickness. The reduction in film thickness results in less separation of the contacting surfaces and therefore more abrasive wear (Stachowiak & Batchelor, 2014: 11).

The effect due to solid particles (LFO)

The wear scars for filtered LFO and unfiltered LFO under oxygen-rich atmosphere look similar with filtered LFO having less abrasive wear due to the removal of solid particles. The solid particles interact with the surfaces which results in increase in CR and more wear.

Effect of atmosphere (LFO)

Abrasive wear slightly decreases for LFO under oxygen-rich atmosphere when compared with LFO under nitrogen atmosphere. The oxygen-rich atmosphere improves the lubricating film (better separation of oscillating ball and disc specimen) of LFO due to the formation of a protective layer (ferrous oxide) which protects the contacting surface when compared with nitrogen atmosphere. (Liu & Xue, 1997).

4.5.1.4 Wear scar diameter (LFO)

The corrected wear scar diameters ($WS_{1.4}$) produced from the friction and wear tests are shown below. The error bars indicate the spread of the triplicate repeats for each condition.

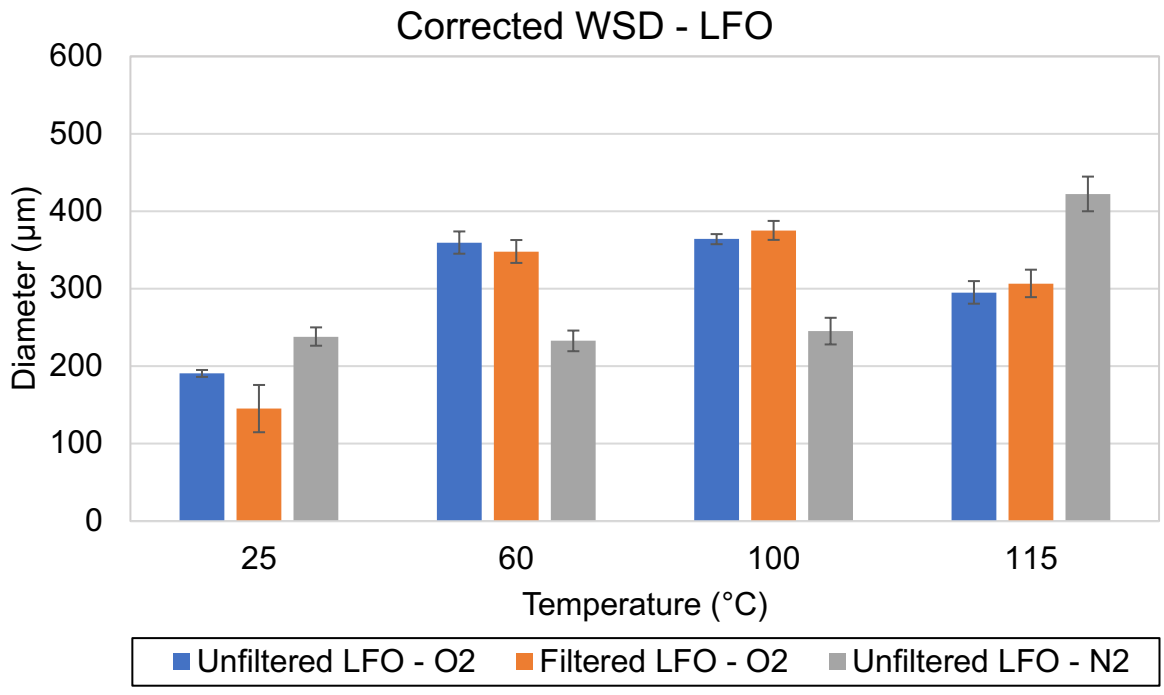

Figure 25: Average wear scar diameter for LFO.

The effect of temperature (LFO)

Figure 25 shows the average corrected wear scar diameter ($WS_{1.4}$) for LFO at different temperatures. For unfiltered LFO and filtered LFO under oxygen-rich atmosphere, the increase in temperature results in the increase in $WS_{1.4}$, although there is a decrease between 100 and 115 °C. The increase in $WS_{1.4}$ for LFO is due to the decrease in viscosity with increasing temperature which results in the less resistance to shear and

decrease in film thickness. This causes the ball and disk to move closer together resulting in increased $WS_{1.4}$ (Stachowiak & Batchelor, 2014). For unfiltered LFO under nitrogen atmosphere, the $WS_{1.4}$ remains stable between 25 and 100 °C, although there is a drastic increase between 100 and 115 °C. This trend is also shown by COF results shown in Figure 24(i)-(l).

The effect due to solid particles (LFO)

At 25 °C, filtered LFO under oxygen-rich atmosphere has lower $WS_{1.4}$ when compared with unfiltered LFO under oxygen-rich atmosphere. For 60 to 115 °C, there is minimal change in $WS_{1.4}$ with increasing temperature.

The effect of atmosphere (LFO)

At 25 and 115 °C, unfiltered LFO under oxygen-rich atmosphere has lower $WS_{1.4}$ when compared with unfiltered LFO under nitrogen atmosphere, although at 60 and 100 °C, unfiltered LFO under oxygen-rich atmosphere has higher $WS_{1.4}$ when compared with unfiltered LFO under nitrogen atmosphere.

4.5.2 MFO

4.5.2.1 Coefficient of friction (MFO)

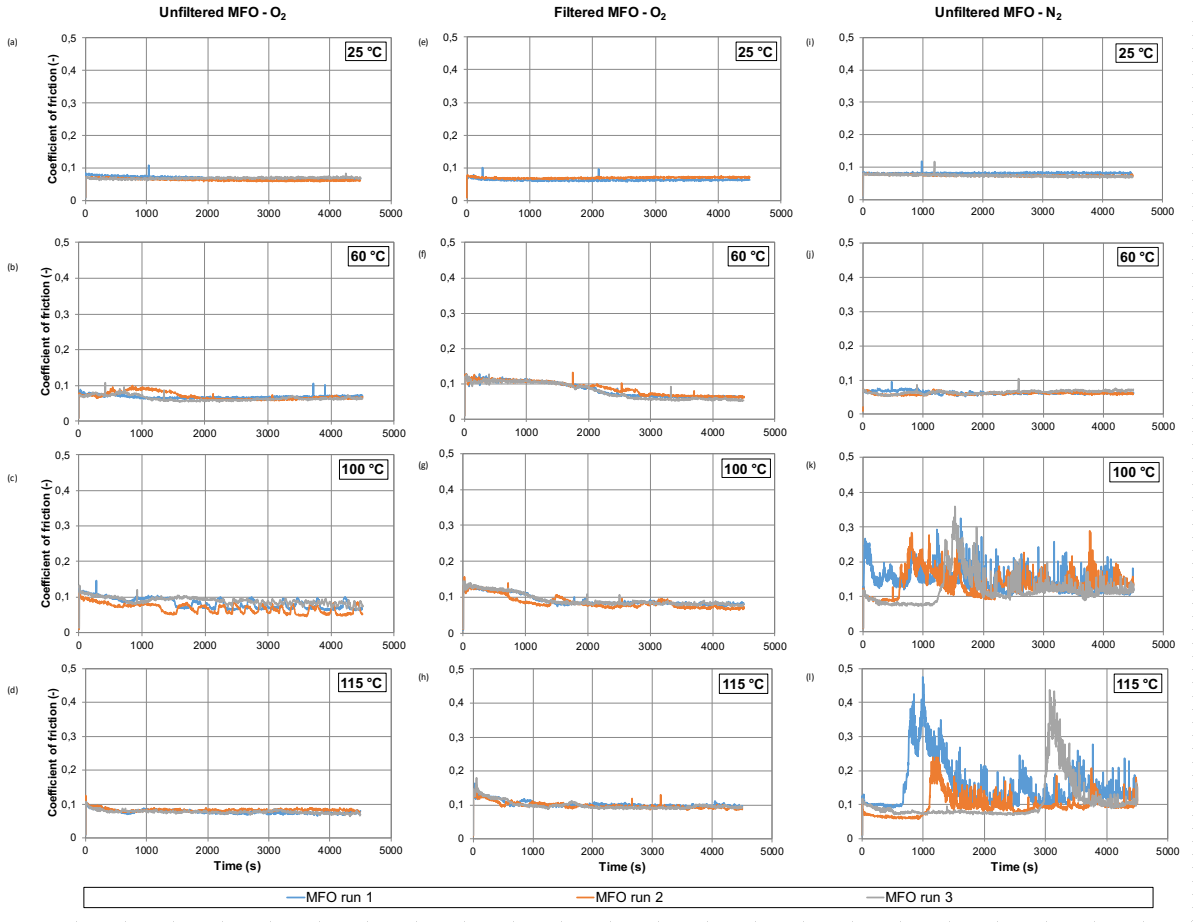

Figure 26: Coefficient of friction versus time graphs of MFO for three runs at different temperatures.

The effect of temperature (MFO)

The increase in temperature for unfiltered MFO and filtered MFO under oxygen-rich atmosphere results in decreased stability of the COF, although there is an increase between 100 to 115 °C shown in Figure 26(a)-(h). At 25 °C, the low temperature limits chemical wear taking place because there is minimal frictional heat present but as temperature increases the protective layer is more likely to be rubbed away due to increased frictional heat resulting in the instability of COF (Garaniya et al, 2018; Bhushan, 2013: 359).

The increase in temperature for unfiltered MFO under nitrogen atmosphere results in the decrease in COF between 25 and 60 °C. At 100 and 115 °C, the COF values

fluctuate throughout the test with high COF values and high COF peaks. The COF values at 115 °C are much higher than those at 100 °C. The high and rough COF profile could be due to the breakthrough of the fuel oil; this will be confirmed by the wear results. MFO contains asphaltenes and solid particles. At high temperatures, the effect of atmosphere is prominent. Adsorption is temperature dependent and reduces at high temperatures and therefore less protection of the metal surfaces (Pawlak, 2003: 161).

The effect of asphaltenes (MFO)

There is minimal change in COF for filtered MFO and unfiltered MFO under oxygen-rich atmosphere at different temperatures. Asphaltenes and some waxes were removed during the filtration process for MFO. Waxes have good lubricating properties and removal of some waxes and asphaltenes resulted in no apparent effect in COF when compared with unfiltered MFO under oxygen-rich atmosphere. The asphaltenes are very polar compounds which adsorb on the metal surface resulting in formation of a protective layer. This results in similar COF values for unfiltered MFO and filtered MFO under oxygen-rich atmosphere with smoother profile for filtered MFO due to removal of asphaltenes and solid particles.

The effect of atmosphere (MFO)

The increase in temperature between 25 and 60 °C for unfiltered MFO under oxygen-rich atmosphere and nitrogen atmosphere results in minimal change in the COF. At 100 and 115 °C, the COF is significantly lower for unfiltered MFO under oxygen-rich atmosphere when compared with unfiltered MFO under nitrogen atmosphere. At high temperatures, the effect of atmosphere is prominent. The nitrogen inert atmosphere has much less oxygen than the oxygen-rich atmosphere. The lower COF under oxygen-rich atmosphere is due to formation of a protective layer (ferrous oxide) which protects the contacting surface resulting in reduced COF when compared to unfiltered MFO under nitrogen atmosphere. The lack of oxide formation results in less protection of the surface and increased COF for unfiltered MFO under nitrogen atmosphere (Pawlak, 2003: 161).

4.5.2.2 % Film thickness (MFO)

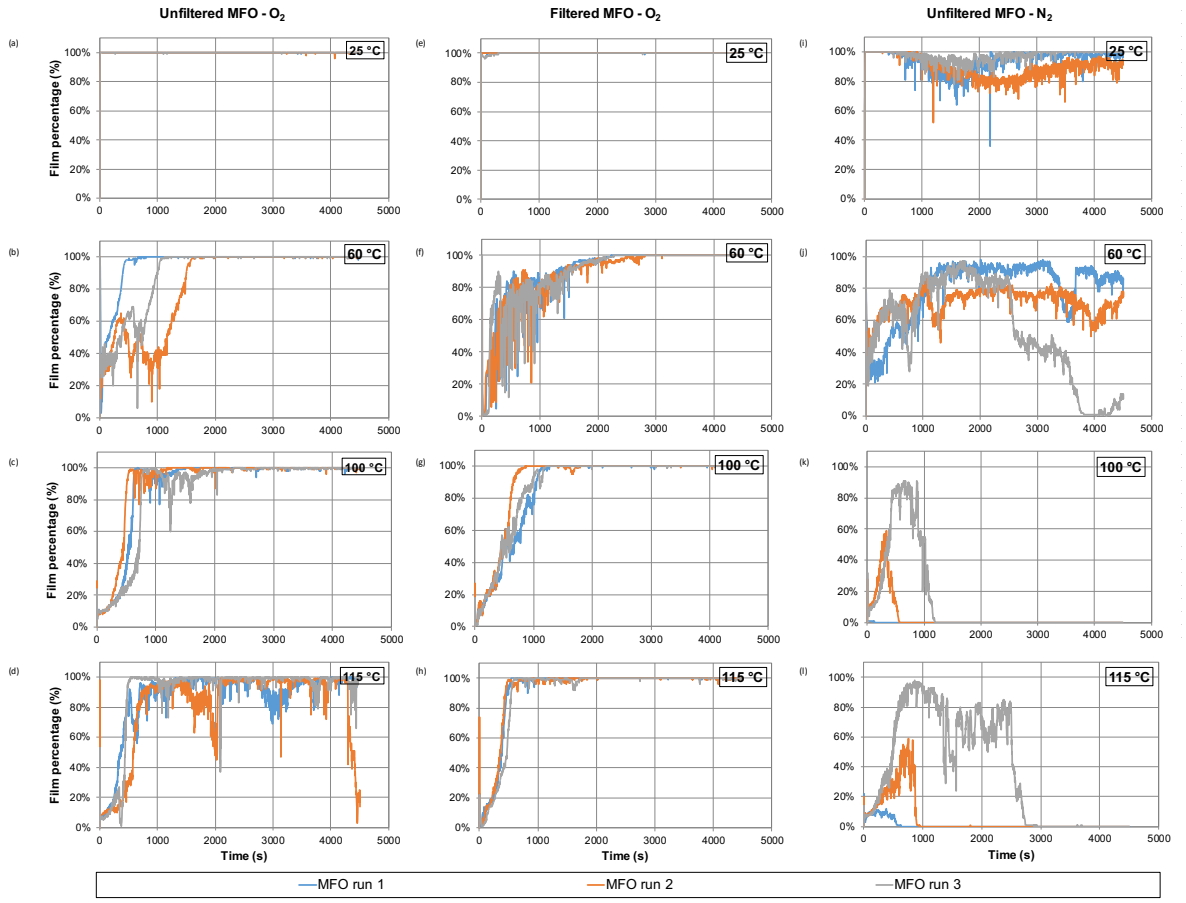

Figure 27: Film versus time graphs of MFO for three runs at different temperatures.

Effect of temperature (MFO)

For unfiltered MFO and filtered MFO under oxygen-rich atmosphere, the increase in temperature shows minimal change in the % film shown in Figure 27(a)-(h). The % film increases to 100%. For unfiltered MFO under oxygen-rich atmosphere, the increase in temperature results in film instability without % film breakdown. Metal particles in the unfiltered MFO under oxygen-rich atmosphere, mainly Fe can oxidise during the tribological layer leading to unstable electrical resistance between the metallic surfaces, the degree of oxidation increases with increasing temperature (Anand *et al*, 2015; Hudedagaddi *et al,* 2017). For filtered MFO under oxygen-rich atmosphere, the roughness between 60 to 115 °C decreases as the test progresses while at 25 °C the % film is smooth.

The increase in temperature for unfiltered MFO under nitrogen atmosphere results in the decrease in % film and relatively constant % film roughness (rough profiles). For 100 and 115 °C, the % film peaks and drops to zero which could be a result of removal of metal oxide and therefore metal-to-metal contact occurs namely breakthrough. This will be confirmed by the wear results. The % film peaks occur at different times in the tests which is shown by the different film peaks. Initial peaks can be attributed to the presence of a thin film of metal oxide on the surface that breaks down at different times due to different film thickness (Viesca, 2010). This can be concluded by the COF profile which shows instability in COF at different times.

Effect of asphaltenes (MFO)

The % film shows minimal change for filtered and unfiltered MFO at different temperatures.

Effect of atmosphere (MFO)

For unfiltered MFO under nitrogen atmosphere, results show a decrease in % film when compared with the unfiltered MFO under oxygen-rich atmosphere at different temperatures. The % film at 100 and 115 °C decreases to a % film of zero under nitrogen atmosphere, while under oxygen-rich atmosphere the % film is at 100% with film breakdown at 115 °C in comparison with 100 °C. The unfiltered MFO under nitrogen atmosphere decreases to zero film at 60 °C for run 3 due to the presence of asphaltenes in MFO which results in unrepeatable % film results. MFO contains asphaltenes which are semi solid (sticky) and could result in zero film if glued to the ball and disk during the test due to its high polarity. This is confirmed by the repeatable stable COF shown in Figure 26(j).

4.5.2.3 Wear scar micrographs (MFO)

Table 12: Wear scars for MFO at different temperatures.

	25 °C	60 °C	100 °C	115 °C
Unfiltered MFO (O_2)	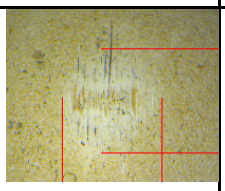	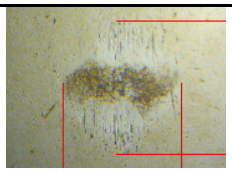	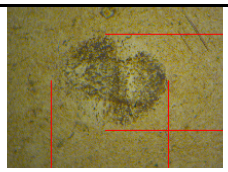	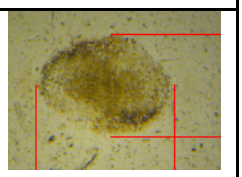
CR	3	3	2	2
$WS_{1.4}$ (µm)	177	191	185	184
Filtered MFO (O_2)	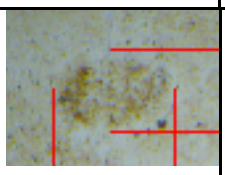	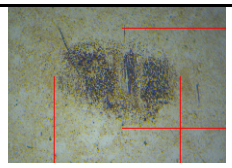	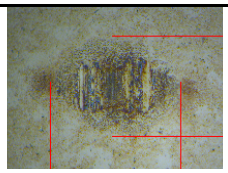	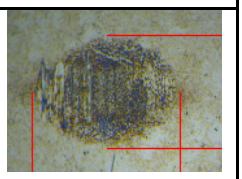
CR	3	2	4	4
$WS_{1.4}$ (µm)	85	206	188	175
Unfiltered MFO (N_2)	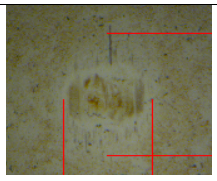	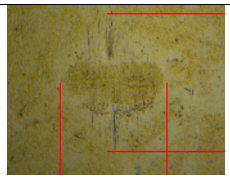	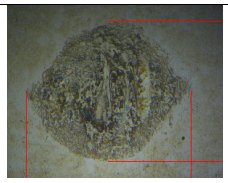	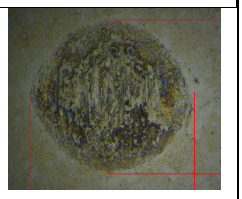
CR	3	3	5	5
$WS_{1.4}$ (µm)	216	229	422	443

The effect of temperature (MFO)

For unfiltered MFO under oxygen-rich atmosphere, the CR stays constant between 25 and 60 °C at a CR of 3, then decreases and stabilizes at a CR of 2. The minimal change in the CR correlates with the minimal change in the COF with increasing temperature. As the temperature increases, the degree of oxidation on the wear scar increases resulting in the formation of a protective layer and therefore a decrease in abrasive wear (Hudedagaddi *et al,* 2017). This is seen by the darkening of the wear scar and less visible scratch lines with increasing temperature (Oláh *et al*, 2005). There is more oxidative wear present in filtered MFO under oxygen-rich atmosphere when compared with unfiltered MFO under oxygen-rich atmosphere with increasing temperature.

For filtered MFO, the increase in temperature results in the increase in abrasive wear and oxidative wear. The CR slightly decreases between 25 and 60 °C and increases between 60 and 100 °C and stabilizes at a CR of 4.

For unfiltered MFO under nitrogen atmosphere, the CR stays constant between 25 and 60 °C at a CR of 3, then increases and stabilizes at a CR of 5. The drastic increase in CR is due to severe abrasive wear and not breakthrough since the CR is not a 6 which is defined as no lubrication. At high temperatures, the film thickness decreases due to decrease in viscosity. The reduction in film thickness resulted in minimal separation of the contacting surfaces at high temperatures and therefore severe abrasive wear present due to the asphaltenes and solid particles interacting with the metal surfaces (Stachowiak & Batchelor, 2014: 11).

The effect of asphaltenes (MFO)

Filtered MFO shows abrasive wear at high temperatures (100 and 115 °C). The removal of some waxes during the filtration of asphaltenes resulted in more wear at high temperatures. The heavy fractions of the MFO, waxes and asphaltenes, play an important role in rheological behaviour of fuel oils (Alcazar-Vara & Buenrostro-Gonzalez, 2011). The presence of waxes can modify asphaltene behaviour, accelerate the dissolution of asphaltenes and modify their stability (Rogel *et al*, 2016). This means the transition of asphaltenes to liquid form is accelerated resulting in much higher viscosity of unfiltered MFO when compared with filtered MFO. This results in better separation between the metal surfaces at 100 and 115 °C therefore less wear taking place.

The effect of atmosphere (MFO)

The CR remains the same for unfiltered MFO under oxygen-rich atmosphere and under nitrogen atmosphere between 25 and 60 °C which shows slight abrasion of metal surface. At high temperatures, the CR of MFO decreases under oxygen-rich atmosphere when compared with nitrogen atmosphere. The oxygen-rich atmosphere results in the reduction of abrasive wear. Severe abrasion under nitrogen atmosphere is present. The oxygen-rich atmosphere improves the lubricating film (better separation of oscillating ball and disc specimen) of MFO due to the formation of a

protective layer (ferrous oxide) which protects the contacting surface when compared with nitrogen atmosphere. (Liu & Xue, 1997).

4.5.2.4 Wear scar diameter (MFO)

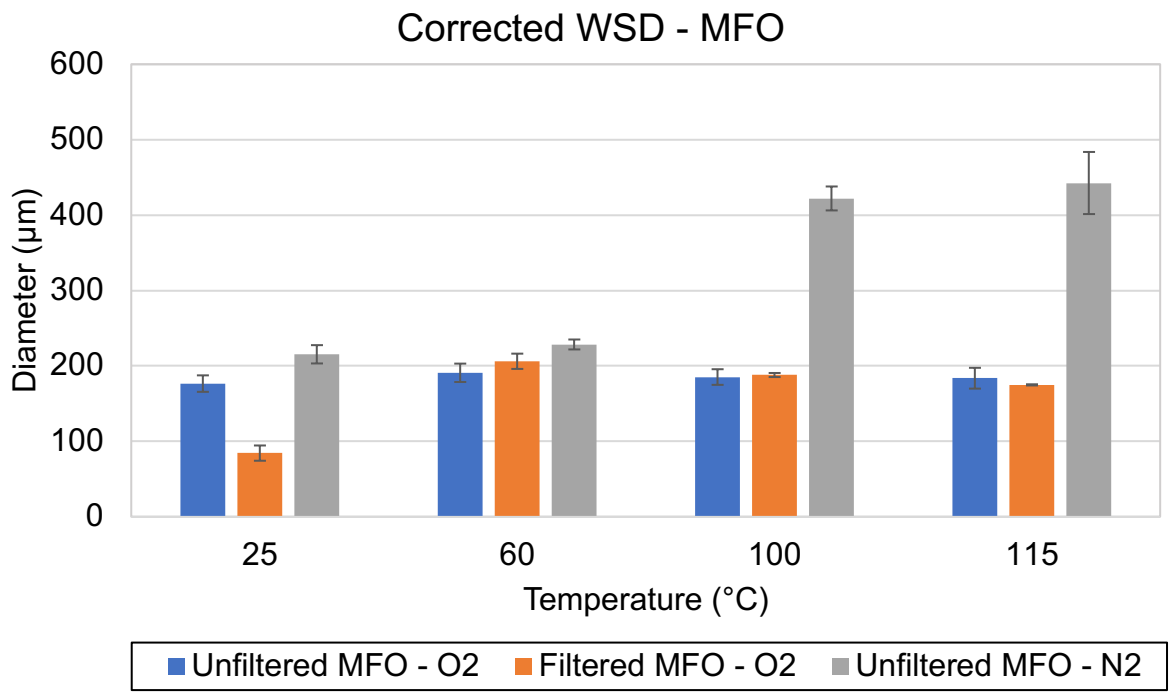

Figure 28: Average wear scar diameter for MFO.

The effect of temperature (MFO)

For unfiltered MFO under oxygen-rich atmosphere, the increase in temperature results in minimal change in the $WS_{1.4}$. For filtered MFO under oxygen-rich atmosphere, there is an increase in $WS_{1.4}$ between 25 and 60 °C, although there is minimal change between 60 and 115 °C. For unfiltered MFO under nitrogen atmosphere, the $WS_{1.4}$ increases with increasing temperature, there is a drastic increase between 60 and 100 °C. This is correlates with the drastic increase in the COF shown in Figure 26(i)-(j) for the infiltered MFO under nitrogen atmosphere.

The effect of asphaltenes (MFO)

At 25 °C, unfiltered MFO under oxygen-rich atmosphere has a higher $WS_{1.4}$ when compared with filtered MFO under oxygen-rich atmosphere. For 60 and 115 °C, there is minimal change in $WS_{1.4}$ for unfiltered MFO and filtered MFO under oxygen-rich atmosphere. This correlates with the COF results shown in Figure 26(a)-(h).

The effect of atmosphere (MFO)

Unfiltered MFO under oxygen-rich atmosphere results in lower $WS_{1.4}$ when compared with unfiltered MFO under nitrogen atmosphere at different temperatures.

4.5.3 HFO

4.5.3.1 Coefficient of friction (HFO)

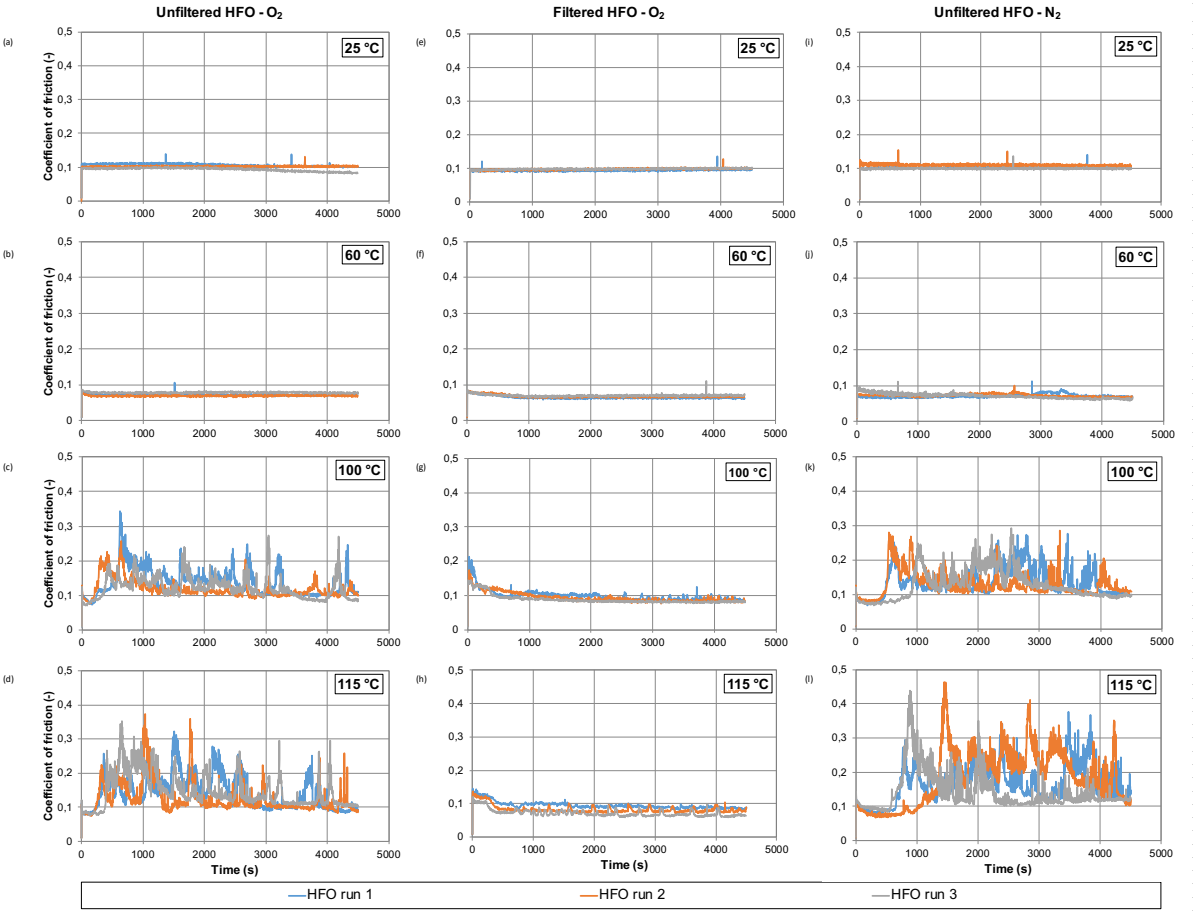

Figure 29: Coefficient of friction versus time graphs of HFO for three runs at different temperatures.

The effect of temperature (HFO)

The COF for filtered HFO and unfiltered HFO under oxygen-rich atmosphere and unfiltered HFO under nitrogen atmosphere shown in Figure 29 decreases between 25 and 60 °C. The lower COF at 25 °C is due to the high viscosity at low temperatures resulting in more power for HFO to be sheared. The power losses are higher and more

heat is generated resulting in increased heat of the contacting surfaces which leads to a higher COF at 25 °C in comparison with 60 °C (Stachowiak & Batchelor, 2014: 11). At lower temperatures (25 and 60 °C), there is more separation of the contacting surfaces due to the high viscosity which results in a thick film in comparison with high temperatures. The thick film results in negligible interactions of the asphaltenes and solid particles in unfiltered HFO and the contacting surfaces.

At 100 and 115 °C, the COF values for unfiltered HFO under oxygen-rich atmosphere and under nitrogen atmosphere fluctuate throughout the test with high COF peaks with the COF values at 115 °C being much higher than those at 100 °C. The high and rough COF at 100 and 115 °C could be due to breakthrough of the fuel oil; this will be confirmed by the wear results. Unfiltered HFO contains a high concentration of asphaltenes and solid particles. At high temperatures the effects of the asphaltenes and solid particles are most prominent due to the drastic decrease in viscosity and therefore the reduction in film thickness, resulting in more interactions between the asphaltenes and solid particles in unfiltered HFO and surfaces. The interactions lead to concentration of heat which increases the COF and results in a rougher COF profile (Stachowiak & Batchelor, 2014: 11). For filtered HFO under oxygen-rich atmosphere, the COF values are low (0.1) at 100 and 115 °C. The removal of abrasive asphaltenes and solid particles during filtration shows significant decrease of the COF.

The effect of asphaltenes (HFO)

At 25 and 60 °C, the COF results for filtered HFO and unfiltered HFO under oxygen-rich atmosphere shows minimal change. HFO is a thick oil and at low temperatures results in good separation of the contacting surfaces due to thick film (Stachowiak & Batchelor, 2014: 11). The effect of asphaltenes and solid particles in HFO is seen at high temperatures (100 and 115 °C) shown by the high and rough COF values.

The effect of atmosphere (HFO)

For unfiltered HFO, the different atmospheric conditions (oxygen-rich and nitrogen atmosphere) result in minimal change in COF. The high concentration of asphaltenes and solid particles in HFO is most prominent in the trend of the COF with increasing temperature and not due to atmosphere.

4.5.3.2 % Film thickness (HFO)

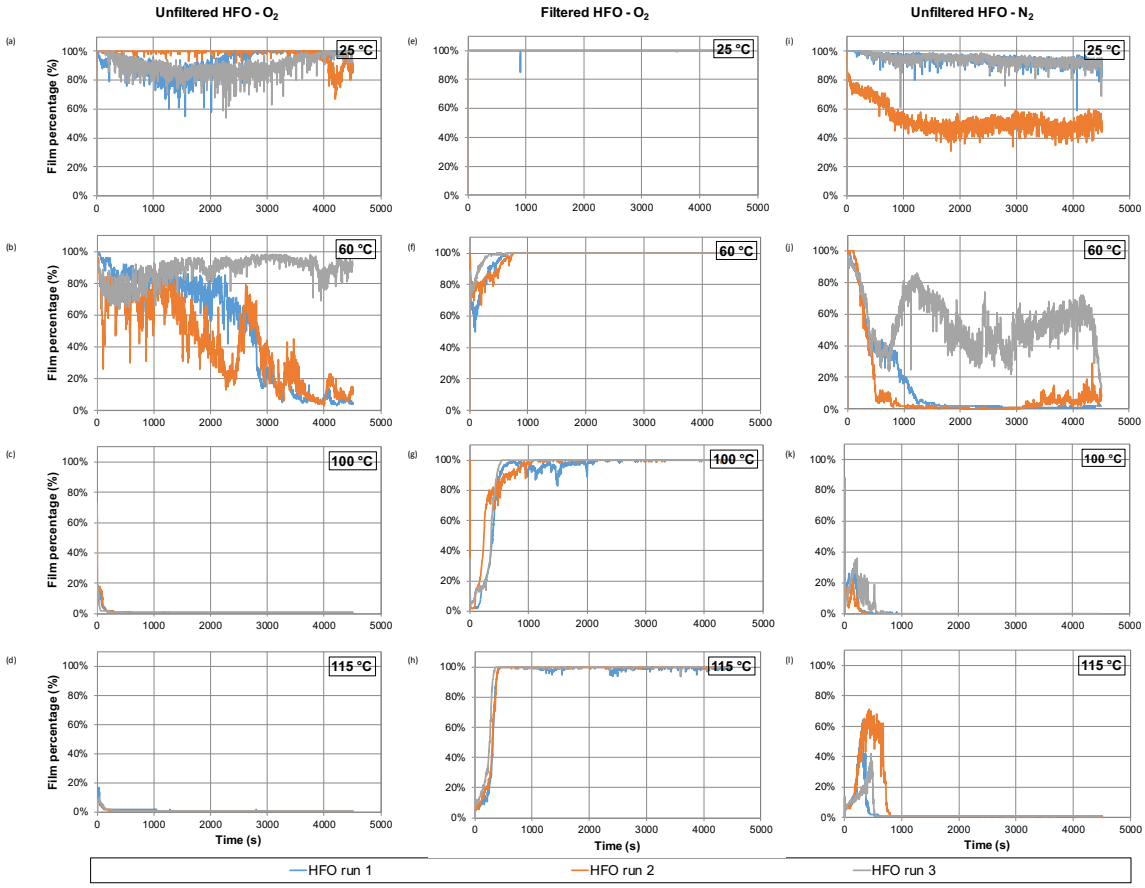

Figure 30: Film versus time graphs of HFO for three runs at different temperatures.

Effect of temperature (HFO)

For unfiltered HFO under oxygen-rich atmosphere and nitrogen atmosphere, the % film decreases as the temperature increases from 25 to 60 °C and has zero film for 100 and 115 °C shown in Figure 30(a)-(d) and Figure 30 (i)-(l). For unfiltered HFO under oxygen-rich atmosphere and nitrogen atmosphere at 25 and 60 °C, the % film shows bad repeatability with rough % film graphs. The asphaltene content in unfiltered HFO is likely to be the cause of bad repeatability in % film. For unfiltered HFO under nitrogen atmosphere at 60 °C, the two runs show the % film decreases to zero but does not result in high COF values which can be shown in the COF results in Figure 29(j).The unfiltered HFO under nitrogen atmosphere having zero film at 60 °C is due to the high concentration of asphaltenes which results in unrepeatable % film results. The HFO has high concentration of asphaltenes which are semi solid (sticky) and could result in zero film if attached to the ball and disk during the test due to its high

polarity. The zero film and high COF for unfiltered HFO under nitrogen atmosphere at 100 and 115 °C could be a result of breakthrough; this will be confirmed by wear results.

For filtered HFO under oxygen-rich atmosphere, the % film is relatively constant with increasing temperature. The % film increases to 100%. The smoothness of the % film decreases with increasing temperature, although it then increases between 100 and 115 °C.

Effect of asphaltenes (HFO)

The % film increases for filtered HFO under oxygen-rich atmosphere when compared with unfiltered HFO under oxygen-rich atmosphere at different temperatures. The increase in % film is due to the removal of asphaltenes which are highly polar. At 100 and 115 °C, the % film is zero for unfiltered HFO under oxygen-rich atmosphere while for filtered HFO under oxygen-rich atmosphere the % film is 100%. The different film results for filtered HFO and unfiltered HFO under oxygen-rich atmosphere could be attributed to the third body behaviour of asphaltenes and solid particles in unfiltered HFO that increases the friction and reduces the electrical conductivity between metal surfaces and therefore less % film (Alves *et al*, 2013).

Effect of atmosphere (HFO)

For 25 and 60 °C, unfiltered HFO under oxygen-rich atmosphere and nitrogen atmosphere shows bad % film repeatability with the % film of unfiltered HFO under nitrogen atmosphere having lower % film. At 100 and 115 °C, the % film for unfiltered HFO under oxygen-rich and nitrogen atmosphere could be a result of breakthrough; this will be confirmed by wear results.

4.5.3.3 Wear scar micrographs (HFO)

Table 5: Wear scars for HFO runs at different temperatures.

	25 °C	60 °C	100 °C	115 °C
Unfiltered HFO	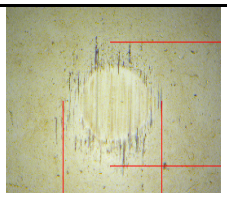	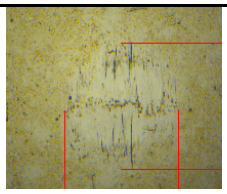	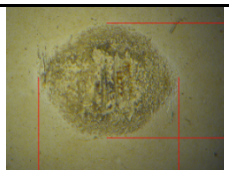	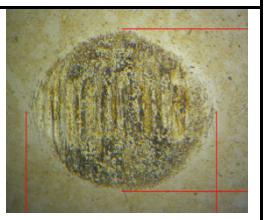
CR	6	3	4	5
$WS_{1.4}$ (µm)	217	222	343	431
Filtered HFO	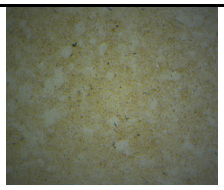	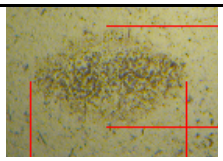	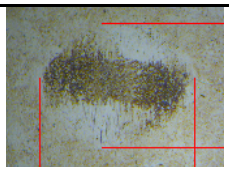	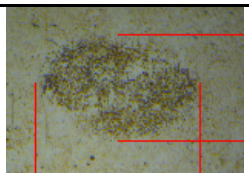
CR	-	3	3	3
$WS_{1.4}$ (µm)	-	137	201	168
Unfiltered HFO (N_2)	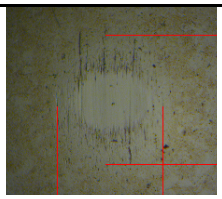	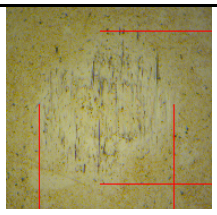	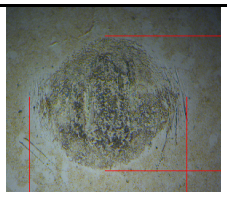	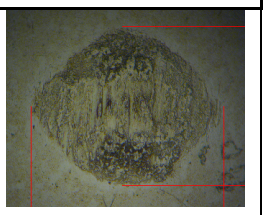
CR	6	3	4	5
$WS_{1.4}$ (µm)	252	282	397	518

The effect of temperature (HFO)

The CR and abrasive wear decrease for unfiltered HFO under oxygen-rich atmosphere and under nitrogen atmosphere with increasing temperature from 25 to 60 °C, although the CR increases between 60 °C to 115 °C. The high abrasive wear at 25 °C is due to the high viscosity at low temperatures resulting in more power for HFO to be sheared. The power losses are higher and more heat is generated resulting in increased heat of the contacting surfaces which leads to more wear (Stachowiak & Batchelor, 2014: 11). As the temperature increases between 60 and 115 °C, the abrasive wear increases due to decrease in viscosity resulting in a thinner film thickness which leads to abrasive particles of asphaltenes and solid particles interacting with the metal surfaces. The high concentration of asphaltenes in HFO

results in asphaltene adsorption at the surface of the metal because of the very polar compounds in asphaltenes. The lower temperature (60 °C) limits chemical wear taking place because there is minimal frictional heat present but as temperature increases the protective layer is more likely to be rubbed away due to increased frictional heat resulting in increased wear (Garaniya *et al,* 2018; Bhushan, 2013: 359). For unfiltered HFO under oxygen-rich atmosphere and under nitrogen atmosphere at 100 and 115 °C, although severe abrasive wear is present . The CR is not a 6 which is defined as no lubrication; therefore we can conclude that unfiltered HFO at 100 and 115 °C does not result in breakthrough but instead results in severe wear.

Filtered HFO has no wear scar at 25 °C, the viscosity is high which results in a thick film capable of separating the two contacting surfaces completely. As the temperature increases between 60 and 115 °C for filtered HFO under oxygen-rich atmosphere, the CR remains constant. The removal of asphaltenes for filtered HFO results in no abrasive wear present. Oxidative wear becomes the dominant wear process which increases with increasing temperature.

The effect of asphaltenes (HFO)

The CR for filtered HFO under oxygen-rich atmosphere is much lower than unfiltered HFO under oxygen-rich atmosphere at different temperatures. This is due to the removal of asphaltenes and solid particles which are highly abrasive and play a major role in the viscosity of the fuel oil.

The effect of atmosphere (HFO)

For HFO, the different environmental conditions (oxygen-rich and nitrogen atmosphere) results in minimal change in wear. The high concentration of asphaltenes and solid particles in HFO is most prominent in the increase in wear with increasing temperature.

4.5.3.4 Wear scar diameter (HFO)

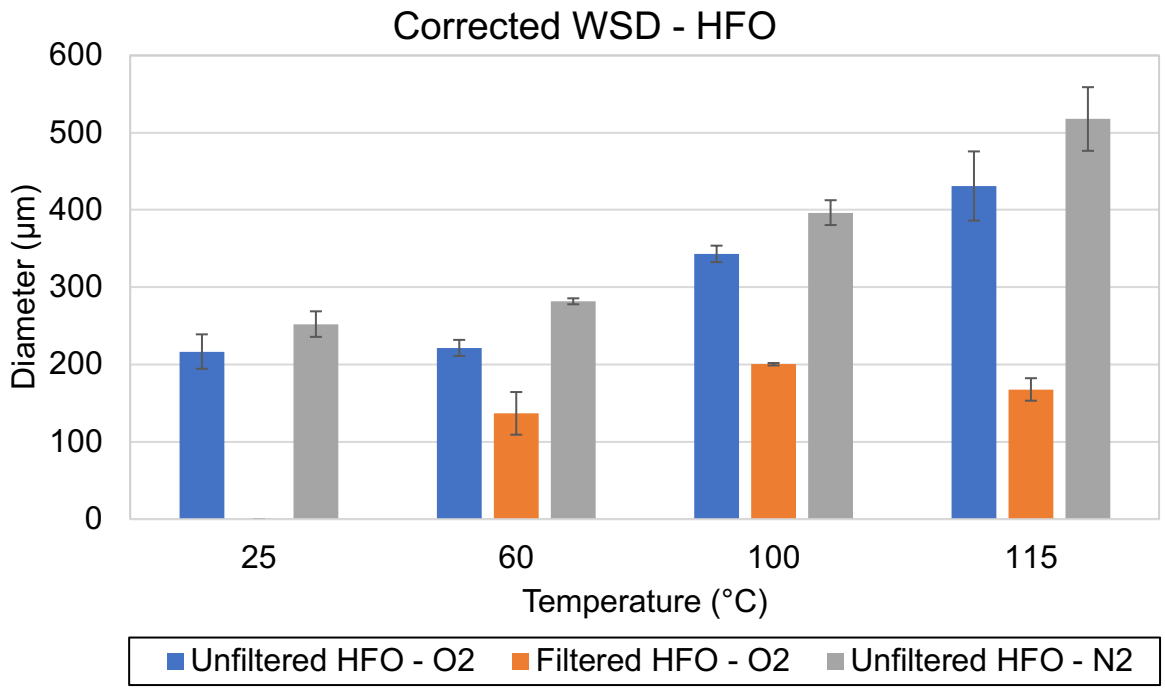

Figure 31: Average wear scar diameter for HFO.

The effect of temperature (HFO)

For unfiltered HFO under oxygen-rich atmosphere and under nitrogen atmosphere, increase in temperature results in the increase in $WS_{1.4}$. At 25 °C, there was no wear scar for filtered HFO under oxygen-rich atmosphere. Filtered HFO has no wear diameter at 25 °C, the viscosity is high which results in a thick film capable of separating the two contacting surfaces completely. For filtered HFO under oxygen-rich atmosphere, the increase in temperature results in increased $WS_{1.4}$, although between 100 and 115 °C there is a decrease.

The effect of asphaltenes (HFO)

At 25 °C, unfiltered HFO under oxygen-rich atmosphere has a $WS_{1.4}$ of around 200 µm while filtered HFO under nitrogen atmosphere has no wear scar. For 60 to 115 °C, unfiltered HFO under oxygen-rich atmosphere has a higher $WS_{1.4}$ when compared with filtered HFO under oxygen-rich atmosphere.

The effect of atmosphere (HFO)

Unfiltered HFO under oxygen-rich atmosphere has a lower $WS_{1.4}$ when compared with unfiltered HFO under nitrogen atmosphere at different temperatures. This confirms what had been observed earlier, namely that the different environmental conditions (oxygen-rich and nitrogen atmosphere) results in minimal change in wear. The high concentration of asphaltenes and solid particles in HFO is most prominent in the increase in wear with increasing temperature.

5 Conclusions and Recommendations

The effect of temperature, asphaltene content and atmosphere were investigated in this work. Lubricity tests were performed on filtered (under oxygen-rich (air) atmosphere) and unfiltered fuel oils (under inert (nitrogen) and oxygen-rich (air) atmosphere). The following conclusions may be drawn:

Effect of asphaltene concentration

- LFO with no asphaltenes (solid particles only) has little impact on the COF and wear from 60 to 115 °C. The trend for COF and wear is similar for both filtered and unfiltered LFO. The solid particles affect the roughness of the COF, minimal change in the $WS_{1.4}$ and slight abrasive wear due to the presence of metals and silica in the solid particles. The removal of solid particles results in minimal change in COF except at 25 °C where the unfiltered LFO has a drastic reduction in COF when compared with filtered LFO. The removal of solid particles in filtered fuel oils under oxygen-rich atmosphere also removes molecules with good lubricity resulting in increased COF when compared with unfiltered LFO under oxygen-rich atmosphere.

- MFO containing high molecular weight paraffin (wax), low concentration of asphaltenes and solid particles resulting in a stable fuel oil. MFO performs better with asphaltenes because the wax stabilizes the asphaltenes resulting in the dissolution of asphaltenes at an accelerated rate. This results in good high temperature performance (less friction and wear at high temperatures). For MFO, the removal of asphaltenes results in minimal change in COF and minimal change in $WS_{1.4}$ from 60 to 115 °C. Due to the presence of waxes in MFO, the wear results for MFO do not follow the typical trend where the increase in temperature usually results in an increase in wear. For MFO, the removal of asphaltenes and solid particles resulted in a decrease in wear at low temperatures and an increase in wear at high temperatures.

- HFO containing high concentrations of asphaltenes and solid particles results in very high COF and severe abrasive wear at high temperatures. At low and moderate temperatures, unfiltered HFO performs comparable to filtered HFO,

while at high temperatures COF, abrasive wear and $WS_{1.4}$ drastically increases when compared with filtered HFO. Overall HFO performs better in the absence of asphaltenes and solid particles due to their abrasive nature particularly at high temperatures.

The effect of chamber atmosphere

- For LFO, the COF shows minimal change with increasing temperature under nitrogen atmosphere while under oxygen-rich atmosphere the COF increases with increasing temperature, although the trend differs at 115 °C for both oxygen-rich and nitrogen atmosphere. The oxygen-rich atmosphere improves the lubricating film (better separation of oscillating ball and disc specimen) of LFO due to the formation of a protective layer (ferrous oxide) which protects the contacting surface when compared with nitrogen atmosphere. Oxidation is predominant in LFO under oxygen-rich atmosphere, the very low oxygen concentration and humidity in the nitrogen atmosphere results in high COF at 115 °C for unfiltered LFO under nitrogen atmosphere due to less protection of the metal surfaces.

- For MFO, under an oxygen-rich atmosphere this results in a more stable fuel oil. There is minimal change in the COF, wear and WSD with increasing temperature. For MFO, at low and moderate temperatures there is minimal change in the COF and wear with a change in environmental atmosphere. At high temperatures, wear increases drastically under nitrogen atmosphere when compared with oxygen-rich atmosphere. The oxygen-rich atmosphere improves the lubricating film (better separation of oscillating ball and disc specimen) of MFO due to the formation of a protective layer (ferrous oxide) which protects the contacting surface resulting in reduced COF and wear when compared with nitrogen atmosphere.

- For HFO, the high concentration of asphaltenes content results in minimal change in the COF and wear with a change in environmental atmosphere. The poor lubricity of HFO is predominantly due to the asphaltenes and solid particles in HFO.

The presence of asphaltenes changes the viscosity behaviour of fuel oils. Viscosity measurements of filtered fuel oils would be recommended in order quantify the change in viscosity for the fuels oils due to the presence of asphaltenes. Friction and wear tests on filtered fuels under nitrogen atmosphere would be recommended in order to show the effect of atmospheric conditions on friction and wear behaviour for filtered fuel oils and how the results are when compared with the effect of atmospheric conditions for unfiltered fuel oils.

Two perfectly stable fuel oils can be incompatible resulting in atmospheric sludge precipitation when mixed. In addition, two fuels may be compatible at some mixing ratios and not compatible at other mixing ratios, or two fuel oils can be compatible or incompatible over the entire mixing ratio. LFO could possibly be mixed with either MFO or HFO to reduce the viscosity because the main use of LCO is as a blending component in heavy fuel oils for viscosity adjustments in order to reduce the final viscosity of heavy fuel oils. This should be confirmed. Dispersants can be used to control the compatibility problems which could possibly arise (Srivastava & Hancsók, 2014: 347). Filtration of HFO should be performed before use for better performance because filtered HFO results in better lubrication due to removal of abrasive particles resulting in reduced friction and wear and to avoid sediment deposition. Filtration of LFO and MFO is not required before use. Unfiltered LFO and MFO have good lubricating properties and much less particles when compared with HFO. Filtering LFO results in minimal change in lubrication and filtered MFO results in worse lubrication when compared with unfiltered MFO due to the removal of waxes which have good lubricating properties.

Fuel oils pass through pumps, filters, nozzles and other equipment before reaching the burner section. Fuel oils at lower temperatures protect the equipment from premature wear and breakdown of equipment because there is less concentration of heat on the metal surfaces in comparison with higher temperatures. Pumping unfiltered HFO and unfiltered MFO at lower temperatures may result in a much longer pumping period and require more power for the fuel oil to reach the burner section due to high viscosity of HFO and MFO as a result of the presence of asphaltenes. LFO can be pumped to reach the burner section without any problems due to low viscosity, low concentration of particles and the absence of asphaltenes. The fuel oils should not be preheated to high temperatures because more energy is required to preheat the fuel

oils to a higher temperature than a lower temperature and better lubrication at lower temperatures. LFO, MFO and HFO should be used in an oxygen-rich air atmosphere because the environment allows for better lubricity due to less friction and wear when compared with an inert environment. This is due to oxidation of the metal surfaces resulting in better protection of the metal surfaces.

In conclusion, It is recommended that unfiltered LFO be used at lower temperatures (25-60 °C) for best performance and HFO should be filtered before use at lower temperatures (25-60 °C) for best performance. Unfiltered MFO should be used at 60 °C because MFO requires to be preheated before use to avoid the wax solidifying in the equipment.

6 References

Abdullah, M, Malik, SR, Iqbal, MH, Sajid, MN, Shad, NA, Hussain, SZ, Razzaq, W, Javed, Y (2018) “Sedimentation and stabilization of nano-fluids with dispersant”, *Colloids and Surfaces,* 554, 86-92.

Adams, HL, Garvey, M, Ramasamy, US, Ye, Z, Martini, A, Tysoe, WT (2015) ”Shear-induced effects in boundary film formation on copper”, paper presented at The Eleventh International Tribology Conference of the South African Institute of Tribology, 10-12 March, 2015, Pretoria, South Africa.

Agarwal, S, Chhibber, VK, Bhatnagar, AK (2013) “Tribological behaviour of diesel fuels and the effect of anti-wear additives”, *Fuel*, 106, 21-29.

Alcazar-Vara, LA, Buenrostro-Gonzalez, E (2011) “Characterization of the wax precipitation in Mexican crude oils”, *Fuel Processing Technology*, 92, 2366-2377.

Al Fanar Petroleum Oil Trading (*sa*),”Fuel oil also known as heavy fuel oil, marine oil, and furnace oil”, https://alfanarpetroleum.com/fuel-oil/ [2022,February 23].

Altoé, R, de Oliveira, MCK, Lopes, HE, Cirilo, LCM, Lucas, EF, Gonzalez, G (2014) “Solution behaviour of asphaltic residues and deasphalted oil prepared by extraction of heavy oil”, *Colloids and Surfaces A: Physicochemical and Engineering Aspects*, 445, 59-66.

Ancheyta, J, Trejo, F, Rana, MS (2009) *Asphaltenes Chemical Transformation during Hydroprocessing of Heavy Fuel Oils,* CRC Press, Boca Raton.

ASTM D396-18a, 2018 “Standard specifications for fuel oils”.

ASTM D6217-18, 2018 “Standard test method for particulate contamination in middle distillate fuels by laboratory filtration”.

ATSDR (2014) “Toxicological profile for fuel oils” https://www.atsdr.cdc.gov/toxprofiles/tp75-c3.pdf [2018,October 1].

Bosman, R, Hol, J, Schipper, DJ (2011) “Running-in of metallic surfaces in the boundary lubrication regime”, *Wear,* 271, 1134-1146.

Bhushan, B (2013) *Introduction to Tribology*, 2nd edition, Wiley, West Sussex.

Cao, Z, Zhang, X, Xu, C, Huang, X, Wu, Z, Peng, C, Duan, A (2021) “Selective Hydrocracking of light cycle oil into high-octane gasoline over bi-functional catalysts”, *Journal of Energy Chemistry*,52, 41-50.

Chandio, ZA, Ramasamy, M, Mukhtar, HB (2015) “Temperature effects on solubility of asphaltenes in crude oils”, *Chemical Engineering Research and Design,* 94, 573-583.

Curl, H, O’Donnell, K (1977) “Chemical and physical properties of refined petroleum products” https://repository.library.noaa.gov/view/noaa/11031/noaa_DS1.pdf [2018,August 20].

Doustdar, O, Wyszynski, ML, Mahmoudi, H, Tsolakis, A (2016) “Enhancing the properties of Fischer-Tropsch fuel produced from syngas over Co/SiO2 catalyst: Lubricity and calorific value”, *Materials Science and Engineering,* 148, 1-10.

Elbaz, AM, Khateeb, AA, Roberts, WL (2018) “PM from the combustion of heavy fuel oils”, *Energy,* 152, 455-465.

Engelhardt, C, Witzig, J, Tobie, T, Stahl, K (2017) “Influence of water contamination in gear lubricants on wear and micro-pitting performance of case carburized gears”, 69, 612-619.

Garaniya, V, McWilliam, D, Goldsworthy, L, Ghiji, M (2018) “Extensive chemical characterization of a heavy fuel oil”, *Fuel*, 227, 67-78.

Ghanavati, M, Shojaei, M, Ramazani, A (2013) “Effects of asphaltenes content and temperature on viscosity of Iranian heavy crude oil: Experimental and modelling study”, *Energy Fuels*, 27, 7217-7232.

Harker, JH, Allen, DA (1972) *Fuel Science,* Oliver & Boyde, Edinburgh.

Hemmati-Sarapardeh, A, Dabir, B, Ahmadi, M, Mohammadi, AH, Husein, MM (2018) "Toward mechanism understanding of asphaltene aggregation behaviour in toluene: The roles of asphaltene structure, aging time, aging time, temperature and ultrasonic radiation", *Journal of Molecular Liquids,* 264, 410-424.

Himmelblau, DM, Riggs, JB (2013) *Basic Principles and Calculations in Chemical Engineering*, Pearson, New Jersey.

Hudedagaddi, CB, Raghav, AG, Tortora, AM, Veeregowda, DH (2017) "Water molecules influence in the lubricity of greases and fuel", *Wear*, 376-377, 831-835.

Husin, H, Aman, Z, Chyuan, OH (2018) "Correlation between rate of decomposition and temperature of asphaltenes", *Materials Today: Proceedings,* 5, 22128-22136.

ISO 12156-1 (2006) "Diesel fuel - Assessment of lubricity using the frequency reciprocating rig (HFRR)''.

ISO 12156-1 (2018) "Diesel fuel – Assessment of the lubricity using the high-frequency reciprocating rig (HFRR)".

ISO 8217 (2017) "Petroleum products-Fuels (Class F) –specifications of marine fuels".

Kauzlarich, JJ, Williams, JA (2001) "Archard wear and component geometry", *The Proceedings of the Institution of Mechanical Engineers,* 215, 387-403.

Kirk, AD (2015) "The cause and effect of particle agglomeration in high pressure diesel injection systems", paper presented at The Eleventh International Tribology Conference of the South African Institute of Tribology, 10-12 March, 2015, Pretoria, South Africa.

Lapuerta, M, Sánchez-Valdepenas, Ekarong, S (2014) "Effect of ambient humidity and hygroscopy on the lubricity of diesel fuels", *Wear,* 309, 200-207.

Lapuerta, M, Sánchez-Valdepenas, J, Bolonio, D, Sukjit, E (2016) "Effect of fatty acid composition of methyl and ethyl esters on the lubricity at different humidities", *Fuel*, 184, 202-210.

Lei, Y, Han, S, Zhang, J (2016) “Effect of the dispersion degree of asphaltene on wax deposition in crude oil under static conditions”, *Fuel Processing Technology,* 146, 20-28.

Lindner, M (2013), “Oil condition monitoring using electrical conductivity”,

https://www.machinerylubrication.com/Read/29407/oil-condition-monitoring [2022,June 8]

Litzke, W (2004) “A Guide to fuel performance”, ‘Brookhaven National Laboratory’ report to the National Oilheat Research Alliance, Alexandria.

Liu, W, Xue, Q (1997) “Friction and wear of the film formed in an oil immersion test under a nitrogen atmosphere”, *Thin Solid Films,* 295, 19-23.

Mang, T, Dresel, W (2017) *Lubricants and Lubrication,* 3rd edition, Wiley, Weinheim.

Martinez, I (2018) “Fuel properties”, http://webserver.dmt.upm.es/~isidoro/bk3/c15/Fuel%20properties.pdf [2018, August 20].

Mettler-Toledo (2012) “Introduction to Karl Fischer titration”, KF Guide 1, Switzerland.

Mettler-Toledo (2012) “Sample preparation for Karl Fischer titration”, KF Guide 2, Switzerland.

Mullins, OC (2016) “Asphaltenes”,

https://www.slb.com/-/media/files/oilfield-review/defining-asphaltenes.ashx [2018, November 20].

Nickels, L (2011) “Low fuel lubricity in thin distillates”, *World Pumps,* 2, 10.

Oláh, ZS, Szirmai, G, Resofszki, G (2005) “Micro and Macro analyses of wear scar surfaces- A complementary rating method to the evaluation of HFRR test results; International colloquium”, TAE, Ostfildern.

Pasadakis, N, Karonis, D, Mintza, A (2011) ”Detailed compositional study of the light cycle oil (LCO) solvent products”, *Fuel Processing Technology*, 92, 1568-1573.

Pawlak, Z (2003), *Tribochemistry of lubricating oils,* Elsevier, Amsterdam.

PCS Instruments (2020) “HFRR high frequency reciprocating rig”, https://pcs-instruments.com/wp-content/uploads/2014/03/HFRR_Brochure_English.pdf [2018, October 1].

PCS Instruments (2020) “HFRR standard specimen pack ”, https://pcs-instruments.com/product/hfrr-specimens/ [2022, February 22].

PCS Instruments, 2005, *HFRR Installation and Test Preparation Manual*, Hardware Version 1, London.

Rogel, E, Ovalles, Cesar, Vien, Janie, Moir, M (2016) “Asphaltenes characterisation of paraffinic crude oils”, *Fuel*, 178, 71-76.

Rotronic (2005) *The Rotronic Humidity Handbook*, Rotronic Humidity Corporation, New York.

SANS 346, 2016 “Automotive fuels-Requirements and test methods for diesel”.

Scaccia, S (2005) “Water Determination in composite PEO-based polymer electrolytes by volumetric Karl Fischer titration method”, Talanta, 67, 678-681.

Shaffer, S (2014) “Generating a stribeck curve in a reciprocating test (HFRR/SRV-type test)”, https://www.bruker.com/fileadmin/user_upload/8-PDF-Docs/SurfaceAnalysis/TMT/ApplicationNotes/AN1004_RevA2_Generating_a_Stribeck_Curve_in_a_reciprocating_Test-AppNote.pdf [2018, October 1].

Srivastava, SP, Hancsók, J (2014) *Fuels and Fuel-Additives*, Wiley, New Jersey.

Stachowiak, GW, Batchelor, AW (2014) *Engineering Tribology*, 4th edition, Butterworth-heinemann, Oxford.

Soltanahmadi, S, Morina, A, van Eijk, MCP, Nedelcu, I, Neville, A (2017) “Tribochemical study of micropitting in tribocorrosive lubricated contacts: The influence of water and relative humidity”, *Tribology International,* 107, 184-198.

Tekie, HA, McCrindle, RI, Marais, PJJG, Ambushe, AA (2015) “Evaluation of six sample preparation methods for determination of trace metals in lubricating oils using inductively coupled plasma-optical emission spectrometry”, *South African Journal of Chemistry,* 68, 76-84.

Ualberta (*sa)* “What are asphaltenes in petroleum, oilsands, and heavy oil”, https://sites.ualberta.ca/~gray/Links%20&%20Docs/Asphaltenes%20web%20page.pdf [2018, November 20].

Viesca, JL, Hernández Battez, A, González, Reddyhoff, T, Torres Pérez, A, Spikes, HA (2010) “Assessing boundary film formation of lubricant additivised with 1-Hexyl-3-methylimidazolium tetrafluoroborate using ECR as qualitative indicator”, *Wear*, 269, 112-117.

Wong, SF, Dol, SS, Wee, SK, Chua, HB (2018) “Miri light crude water-in-oil emulsions characterization –Rheological behaviour, stability and amount of emulsions formed”, *Journal of Pretroleum Science and Engineering*, 165, 58-66.

Yen, TF, Chilingarian, GV (2000) *Asphaltenes and Asphalts, 2,* Elsevier, Amsterdam.

Zuo, P, Shijie, Q, Shen, W (2019) “Asphaltenes: Separations, structural analysis and applications”, *Journal of Energy Chemistry*, 34, 186-207.

A. Appendix 1

A.1 Cleaning procedure

A.1.1 Before HFRR test

The apparatus and test specimens were cleaned before performing the HFRR lubricity test. The specimens (upper and lower specimen holders, bolts, tweezers and disks and balls) for the HFRR were cleaned using toluene and acetone. Two beakers were cleaned in order to pour the acetone and toluene required for the cleaning procedure. Two 100 mL beakers were cleaned with hexane and thereafter dried in the oven at 90 °C for two minutes. The beakers were removed from the oven and left to cool down. The beakers were then cleaned using acetone and dried in the oven at 90 °C for two minutes. The beakers were removed from the oven and left to cool down. 80 mL of toluene was poured into the beaker and 80 mL of acetone was then poured into the other beaker.

The cleaning procedure took around 30 minutes. The specimens were bathed in the beaker containing toluene and put into the ultra-sonic bath for 10 minutes. It was ensured that at least two thirds of the ultra-sonic bath was filled with distilled water so the specimens in the beaker are fully submerged in the water. The specimens were removed from the toluene beaker after 10 minutes in the ultrasonic bath and put onto a laboratory dish covered with lab paper towel. The specimens were then dried in the oven for two minutes at 90 °C. The specimens were left to cool down and then bathed in the beaker containing acetone. The beaker containing specimens in acetone was put into an ultra-sonic bath for 10 minutes. After 10 minutes, the specimens were moved from the ultrasonic bath onto the same laboratory dish. The specimens were then dried in the oven for two minutes at 90 °C and then left to cool down.

A.1.2 After HFRR test

Once the HFFR lubricity test was complete, the specimens were cleaned in order to take micrographs and measurements of the ball and disk. The temperature of the HFRR equipment was left to cool down to below 40 °C before proceeding with the cleaning procedure. Most of the fuel oil was removed with a paper towel and then the lower and upper specimen holders were disassembled from the HFRR. It was ensured that the disk and ball are not removed from the specimen holders because the ball

scar and disk track need to be measured, this helps to locate the ball scar and wear track. 80 mL of hexane was poured into a 100 mL clean beaker and the lower and upper specimen holders were bathed in the beaker containing hexane and then put into the ultrasonic bath for two minutes. The lower and upper specimen holders were removed from the beaker into the laboratory dish covered with paper towel then dried in the oven for two minutes. The specimen holders were left to cool down before cleaning the specimen holders with acetone. Once the acetone was dry, the ball scar and disk track were measured using the microscope.